

# GIFT: Generative Interpretable Fine-Tuning

Chinmay Savadikar<sup>1</sup>      Xi Song<sup>2</sup>      Tianfu Wu<sup>1</sup>

<sup>1</sup>Department of ECE, North Carolina State University, <sup>2</sup>An Independent Researcher  
`{csavadi, tianfu_wu}@ncsu.edu`

Project Page & Code: <https://savadikarc.github.io/gift>

## Abstract

We present Generative Interpretable Fine-Tuning (GIFT) for parameter-efficient fine-tuning (PEFT) of pretrained Transformer backbones, which we show can be formulated as *a simple factorized matrix multiplication* in the parameter space or equivalently in the activation/representation space, and thus embraces built-in interpretability. For a pretrained layer with weights  $\omega \in \mathbb{R}^{d_{out} \times d_{in}}$ , our proposed GIFT learns the fine-tuned weights  $\hat{\omega}$  directly from  $\omega$  as  $\hat{\omega} = \omega \cdot (\mathbb{I} + \phi_{d_{in} \times r} \cdot \psi_{r \times d_{in}})$  where  $\mathbb{I}$  is an identity matrix.  $\Theta = (\phi, \psi)$  collects the learnable parameters of the two linear layers of GIFT with  $r$  being a hyper-parameter.  $\Theta$  can be shared by all layers selected for fine-tuning (e.g., all the Query and Value layers), or can be layer-type specific (e.g., different  $\Theta$ 's used for Query and Value), resulting in significantly fewer trainable parameters compared to the layer-specific Low-Rank Adaptation (LoRA) method. We perform comprehensive evaluations on natural language tasks (commonsense and arithmetic reasoning, instruction tuning, and sequence classification) and computer vision tasks (fine-grained classification). We obtain the best performance and parameter efficiency among baselines on commonsense reasoning and instruction tuning using the Llama family of models and on visual recognition benchmarks using Vision Transformers. We achieve comparable performance on other benchmarks. Notably, compared to LoRA, we obtain 5.9% absolute increase in average accuracy with 53.8 times reduction of parameters on Commonsense170k using Llama-3 (8B), and 5.4% absolute increase in the win rate with 4 times reduction of parameters using Llama-2 (7B) during instruction tuning. Our GIFT also obtains a slightly higher win rate on instruction tuning than GPT 3.5 (Turbo 1106). We show the output of the first linear layer (i.e.,  $\omega \cdot \phi$ ) is surprisingly interpretable, which can play the role of a token-clustering head as a by-product to localize meaningful objects/parts in images for computer vision tasks. Through ablation studies, we verify the effectiveness of the two linear layer formulation by comparing with more sophisticated parameterization schemes. *Our code is available at <https://github.com/savadikarc/gift>.*

## 1 Introduction

Fine-tuning pretrained deep neural networks (DNNs) as feature backbones for downstream tasks, often known as transfer learning, has been an important and challenging research topic in the computer vision and deep learning literature ever since the recent resurgence of DNNs pioneered by the AlexNet [27] trained on the ImageNet-1k dataset [49] in 2012. The goal of fine-tuning DNNs is to transfer knowledge from the pretrained domain/task to facilitate better performance on downstream tasks which otherwise may suffer from not being able to train those DNNs from scratch well due to various considerations such as insufficient amount of data. Fine-tuning DNNs has become a golden standard in practice and shown remarkable progress.

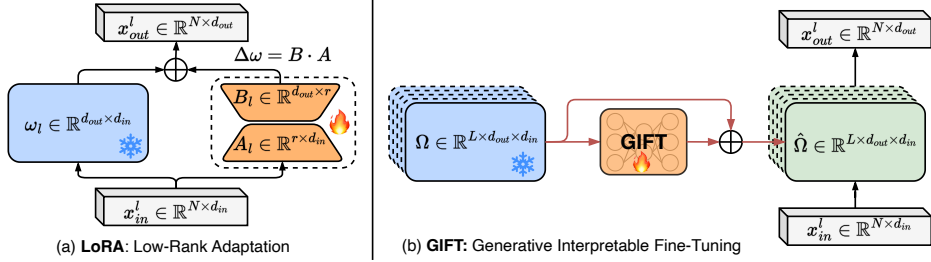


Figure 1: Comparisons between (a) the widely used LoRA [19] and (b) our proposed GIFT. LoRA is a layer-specific fine-tuning paradigm by learning the low-rank weight residuals directly as model parameters in optimization. Our GIFT is a deep weight-residual learning paradigm, which is shared across all the layers of the same type by treating pretrained weights from different fine-tuning layers (e.g.,  $L$ ) as a batch of input “data” and directly computes fine-tuned weights via residual learning. We show that simply parameterizing GIFT with two linear layers (without bias) is surprisingly effective.

To achieve better transferrability, fine-tuning DNNs is not always straightforward by simply updating parameters of a pretrained DNN using a downstream task data (i.e., full fine-tuning). There are subtle details that matter in terms of balancing the exploitation of the pretrained model and the exploration of the new task data [28]: which parts of a pretrained DNN should be fine-tuned, and how should they be trained? More recently, larger and larger feature backbones, so-called large foundation models [4], especially open-source large language models such as Llama [55, 56, 1], have become ubiquitous, while hindering the possibility of training them from scratch, and of fine-tuning them in their entirety for researchers and practitioners who do not have access to high-demanding computing resources. Meanwhile, it may not be even necessary to fine-tune the pretrained model in its entirety due to the aforementioned exploitation-exploration trade-off. To address this issue, parameter-efficient fine-tuning (PEFT) becomes necessary and remains an active research topic.

In this paper, we focus on PEFT of pretrained Transformer backbone models [57, 12], for which the Low-Rank Adaptation (LoRA) [19] is the state-of-the-art method with many follow-up variants. As illustrated in Fig. 1 (a), LoRA learns new model weights in the low-rank form in fine-tuning. Our method is motivated by LoRA, but take a conceptually different perspective to PEFT. The layer-specific low-rank weights (i.e.,  $A_l$  and  $B_l$ ) in LoRA are introduced directly as new model parameters to be optimized in fine-tuning, which do not have direct “information exchange” with the pretrained weights. Instead, we ask: **Can we directly learn the fine-tuned weights from the pretrained weights?**

More importantly, although LoRA and its variants [70, 11, 32, 22, 26, 13, 35] have shown strong performance in PEFT for a wide range of applications, we still lack solid understanding of relationships between the pretrained model and the fine-tuned model beyond their residual connections in the parameter space. For example, we do not have intuitive understanding of the relationship between the learned layer-specific weight residuals  $B_l \cdot A_l$  and the original pretrained weights  $\omega_l$  in LoRA (Fig. 1 (a)). Motivated by this observation, we ask another question: **Can we induce linear relationships between the fine-tuned weight-residuals and the pretrained weights to achieve comparable or even better performance than LoRA on downstream tasks?** If feasible, it simply means that fine-tuning pretrained Transformer backbones can be formulated as a (learned) matrix multiplication in the parameter space, rendering the fine-tuning process with built-in interpretability.

**We show that answers to the above two questions are affirmative in this paper.** Specifically, for a pretrained layer with the weights  $\omega \in \mathbb{R}^{d_{out} \times d_{in}}$ , we show fine-tuned weights  $\hat{\omega}$  can be expressed by,

$$\hat{\omega}_{d_{out} \times d_{in}} = \omega_{d_{out} \times d_{in}} \cdot P_{d_{in} \times d_{in}} = \omega_{d_{out} \times d_{in}} \cdot (\mathbb{I} + \Theta_{d_{in} \times d_{in}}), \quad (1)$$

where  $P_{d_{in} \times d_{in}} = \mathbb{I} + \Theta_{d_{in} \times d_{in}}$ ,  $\mathbb{I}$  an identity matrix and  $\Theta_{d_{in} \times d_{in}}$  a projection matrix to be learned for a downstream task, which is further defined by,

$$\Theta_{d_{in} \times d_{in}} = \phi_{d_{in} \times r} \cdot \psi_{r \times d_{in}}, \quad (2)$$

where  $r$  is a hyper-parameter, playing the role of rank similar in spirit to LoRA. Thus, we can draw intuitive and potentially deeper understanding of PEFT using pretrained Transformer backbones: Pretrained Transformer backbones “distill” general and diverse knowledge from a large-scale pre-training dataset, encoded in the pretrained weights. When fine-tuning them at a downstream task, to

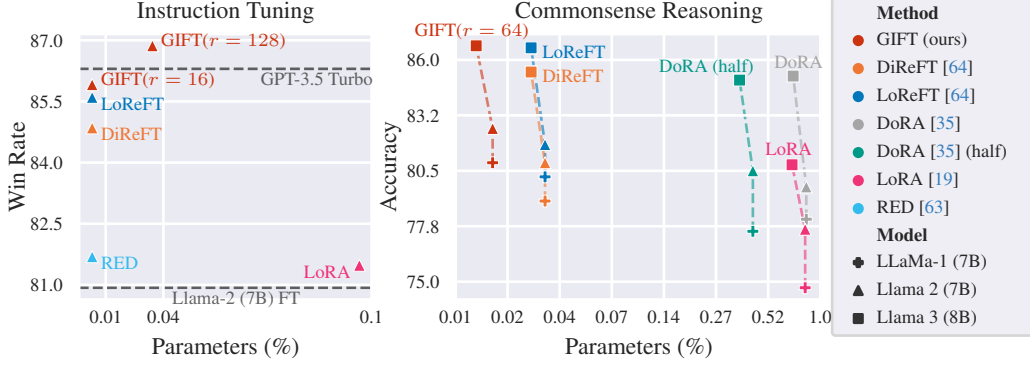


Figure 2: *Left*: Comparisons of win rate vs parameters between different PEFT methods and our proposed GIFT on instruction tuning using the Llama-2 7B [56] model, where the win rate is based on GPT4 evaluation. *Right*: Comparisons of average accuracy vs parameters between different PEFT methods and our proposed GIFT for commonsense reasoning on 8 datasets using the LLaMA-1 7B [55], and LLaMA-2 7B [56] / -3 [1] 8B models. Our GIFT consistently obtains the best performance while using significantly less parameters (see Table 1 and Table 2 for details).

“absorb” new information in the training data of the downstream task, *one of the simplest updates that minimally “distorts” and maximally “preserves” the pretrained knowledge* is defined by Eqn. 1 and Eqn. 2, thanks to the low-rank factorized linear projection in the parameter space. The newly “absorbed” information from the downstream task is also linearly expressed in the space spanned by the pretrained weights (knowledge)  $\omega_{d_{out} \times d_{in}}$  via  $\omega_{d_{out} \times d_{in}} \cdot \Theta_{d_{in} \times d_{in}}$ .

Fig. 1 (b) illustrates the proposed Generative Interpretable Fine-Tuning (GIFT). The simple formulation above is then defined by,

$$\text{GIFT}(\omega; \Theta) = \text{Linear}(\text{Linear}(\omega; \phi); \psi), \quad (3)$$

where  $\Theta$  can be shared by all layers selected for fine-tuning (e.g., all the Query and Value layers), or  $\Theta$  can be layer-type specific (e.g., two different  $\Theta$ ’s used for Query and Value respectively), resulting in significantly fewer trainable parameters compared to layer-specific LoRA.

**How expressive is this simple GIFT?** As seen in Figure 2 (*left*), for instruction following, GIFT obtains better Win Rate against text-davinci using Alpaca-Eval v1.0 [31] than the recently proposed representation fine-tuning method, LoReFT [64], with the same parameter budget using Llama-2, and can perform slightly better than GPT 3.5 Turbo 1106 given more parameter budget which is still 4 times less than LoRA (see Table 1). As shown in Figure 2 (*right*), our GIFT obtains 5.9% absolute increase in average accuracy with 53.8 times fewer parameters on the Commonsense170k reasoning benchmark using Llama-3 in comparison with LoRA. It is also consistently better than LoReFT [64], but using about half the number of parameters (see Table 2).

To understand better what could be learned in our GIFT for downstream tasks, we show that when the GIFT is applied for fine-tuning the projection layers in the multi-head self-attention (MHSA) modules of a pretrained Vision Transformer backbone, the output of the first linear layer in our simple GIFT (Eqn. 3), denoted by,  $C_{d_{out} \times r} = \omega_{d_{out} \times d_{in}} \cdot \phi_{d_{in} \times r}$ , plays the emergent role of a segmentation (a.k.a., token clustering) head for the activation map at the corresponding projection layer in the MHSA, which can localize meaningful objects/parts in testing images of a downstream task (Fig. 3, see Sec. 2.5 for details). These interpretable visualization results emerge as by-product, without any direct supervision signal for these localization capabilities in fine-tuning.

While we show that the fine-tuning weight residuals can be learned as a simple linear function of the pretrained weights, the relationship between them could potentially be non-linear. We explore this through ablation studies using more sophisticated parameterization schemes (Sec. 2.3). In our experiments, we do not observe any significant improvement against our simple two-layer linear parameterization method. We note that when pretrained Transformer backbones are sufficiently expressive, which is often assumed in PEFT, simpler parameterization methods should be more generalizable and better under the principle of Occam’s razor.

**Our Contributions.** We make three main contributions to adapting pretrained Transformer backbones under the PEFT paradigm: (i) We present Generative Interpretable Fine-Tuning (GIFT) that is

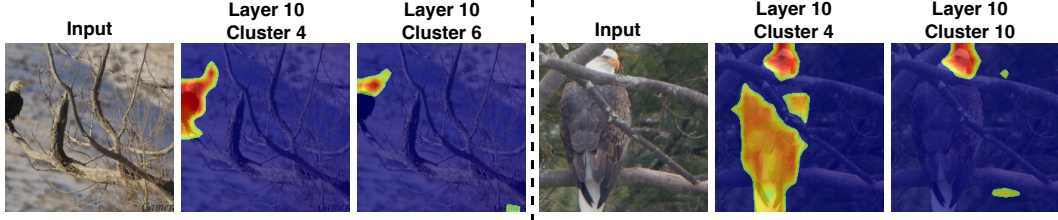


Figure 3: The output of the first linear layer in our GIFT plays the role of a  $r$ -way segmentation/token-clustering head that shows an emergent capability of localizing meaningful objects/parts on images. Two examples from NABirds [17] benchmark in FGVC are shown here with clusters from layer 10 in the ViT-B backbone. More examples can be found in Figure 4 in the Appendix.

conceptually different from the widely used LoRA methods. Our GIFT learns fine-tuned weights directly from the pretrained weights, with its parameters shared by all layers of the same type selected to be fine-tuned, making it even more parameter-efficient than LoRA. (ii) We present a simple parametrization composed of two linear layers for GIFT, which induces simple and interpretable linear relationships between the learned weight-residuals and the original pretrained weights, enabling built-in interpretability. (iii) GIFT parametrized using two linear layers achieves the best accuracy performance and parameter efficiency among baselines in the commonsense reasoning, arithmetic reasoning, and instruction tuning using pretrained Llama family of models, and two computer vision benchmarks (VTAB and FGVC) using ImageNet-21k pretrained ViT-B/16. It also shows emerged visual interpretability in terms of localizing meaningful objects/parts in images. It obtains performance comparable to LoRA on the GLUE benchmark but with less parameters using pretrained RoBERTa-Base/Large.

## 2 Approach

In this section, we first briefly review PEFT and LoRA, and then present our proposed GIFT.

### 2.1 Problem Definition of Parameter-Efficient Fine-Tuning (PEFT)

We consider widely used isotropic pretrained Transformer backbones such as the ViT-B [12] pretrained on the ImageNet-21k [49] and the Llama-2 [56] pretrained on a large text corpus, which will be frozen throughout fine-tuning. The goal of PEFT is to introduce a small number of new parameters which can be estimated using the training data of a downstream task. After estimated, those newly introduced parameters can be integrated into the backbone in one way or another to produce the fine-tuned backbone such as the prompt-based methods [21], bias fine-tuning [66], and the widely used LoRA [19] which aims to fine-tune the pretrained weights (e.g., all Query and Value linear projection layers) to facilitate more expressive fine-tuning with better performance on downstream tasks.

We consider PEFT of weights like LoRA. Denote by  $\Omega$  the set of pretrained weights from a selected subset of layers to be fine-tuned in a pretrained Transformer backbone. Let  $\omega \in \Omega$  be the pretrained weights of a certain selected layer (e.g., a Query linear projection layer). The goal of PEFT is then to learn weight-residuals  $\Delta\omega$  such that the fine-tuned weights can be written as,

$$\hat{\omega} = \omega + \Delta\omega, \quad (4)$$

where  $\Delta\omega$  needs to be parameterized in a way such that the total number of learnable parameters is much smaller than that of the pretrained weights and the peak memory footprint is practically affordable in optimization, to be efficiently estimated using the relatively small training data of a downstream task.

### 2.2 Overview of LoRA

LoRA [19] (Fig. 1 (a)) presents a popular formulation for learning the weight residuals  $\Delta\omega$  using a product of two low-rank parameter matrices  $A \in \mathbb{R}^{r \times d_{in}}$  and  $B \in \mathbb{R}^{d_{out} \times r}$ ,

$$\Delta\omega = B \cdot A, \quad (5)$$

where  $r$  represents the predefined rank (e.g.,  $r = 8$ ). Both  $A$  and  $B$  are treated as model parameters to be learned via optimizing the objective function defined on the downstream task data (e.g., the

cross-entropy loss for classification problems). We omit the subscript  $l$  in  $B$  and  $A$  for notational clarity. The total number of learnable parameters in  $\Delta\omega$  is much smaller than that of the frozen pretrained weights  $\omega$  since both  $d_{in}$  and  $d_{out}$  are often much larger than the predefined low rank  $r$ . During optimization,  $B$  is initialized as a zero matrix, so that Eqn. 5 has no effects before the first parameter update (e.g., for the first mini-batch).

Although strong performance of PEFT has been witnessed using LoRA, we still lack intuitive yet solid understanding of the relationships between  $\Delta\omega$  (Eqn. 5) and the original pretrained weights  $\omega$ .

### 2.3 Our Proposed GIFT

Our proposed GIFT generalizes the parameterization scheme in Eqn. 5 by learning the weight-residual  $\Delta\omega$  directly from the pretrained and frozen weights  $\omega$ ,

$$\Delta\omega = \text{GIFT}(\omega; \Theta), \quad (6)$$

where  $\Theta$  collects the set of parameters of the GIFT network to be trained using a downstream task data. As illustrated in Fig. 1 (b),  $\text{GIFT}(\cdot; \Theta)$  is either layer-agnostic (a.k.a., shared by all layers selected in a pretrained backbone for PEFT) or layer-type-specific (i.e., shared by all layers of the same type, and different for different types of layers).

Let  $\Omega \in \mathbb{R}^{L \times d_{out} \times d_{in}}$  be the pretrained weights from the selected modules (e.g., the linear projection layer in MHSA) across  $L$  blocks of a pretrained Transformer backbone. While training with GIFT, we will term  $L$  the batch size,  $d_{out}$  the number of parameter-tokens, and  $d_{in}$  the dimension of parameter tokens. We propose to parameterize  $\text{GIFT}(\cdot; \Theta)$  as follows,

$$\text{GIFT}(\Omega; \Theta) = \text{Linear}(g(\text{Linear}(\Omega; \phi); \theta); \psi), \quad (7)$$

where we have,

- $\text{Linear}(\Omega; \phi)$  projects the input dimension to a lower dimension (or rank)  $r$  with learnable weights  $\phi \in \mathbb{R}^{d_{in} \times r}$  without bias terms. Denote by  $\Omega_1 \in \mathbb{R}^{L \times d_{out} \times r}$  the output of this dimension-reduction layer.
- $\text{Linear}(\cdot; \psi)$  is an output dimension-recovery projection with learnable weights  $\psi \in \mathbb{R}^{r \times d_{in}}$  and no bias term. Similar to how LoRA initializes the low-rank  $B$ ,  $\psi$  is also initialized as a zero parameter matrix in optimization. It outputs the set of learned weight-residual,  $\Delta\Omega \in \mathbb{R}^{L \times d_{out} \times d_{in}}$ .
- $g(\cdot; \theta)$  is the intermediate sub-network, which can be realized by any suitable network specifications. We consider the following lightweight schema in this paper:
  - **The identity operation:**  $g(\Omega_1; \theta) = \text{Identity}(\Omega_1) = \Omega_1$  with no learnable parameters  $\theta = \emptyset$ , which leads to the simple two-layer linear parameterization of GIFT (Eqn. 1, Eqn. 2 and Eqn. 3), and is the focus in our experiments in this paper.
  - **Element-wise non-linearity functions** without learnable parameters (i.e.,  $\theta = \emptyset$ ): e.g.,  $g(\Omega_1) = \text{Sigmoid}(\Omega_1)$  or  $g(\Omega_1) = \text{GELU}(\Omega_1)$ .
  - **Multi-Layer Perceptrons (MLPs):** e.g.,  $g(\Omega_1; \theta) = \text{Linear}(\text{GELU}(\text{Linear}(\Omega_1; \theta_1)); \theta_2)$ , where  $\theta_1 \in \mathbb{R}^{m \cdot r \times r + m \cdot r}$  and  $\theta_2 \in \mathbb{R}^{r \times m \cdot r + r}$  consist of weights and bias terms of the two linear layers with the MLP latent dimension ratio  $m$  (e.g.,  $m = 2$ ).
  - **Vanilla Transformers:** We treat  $\Omega_1$  as a batch of  $L$  sequences each of which consists of  $d_{out}$  tokens in  $r$ -dim space. We then apply a single vanilla Transformer block [57, 12].
  - **MLP-Mixers:** Similar to vanilla Transformers, we apply a single MLP-Mixer [54] block.

### 2.4 The Built-in Interpretability of Our Two-Linear-Layer Parameterized GIFT

We give a closer comparison of the fine-tuning “behavior” in the parameter space between LoRA and our two-linear-layer parameterized GIFT to highlight our GIFT’s built-in interpretability. Without loss of generality and for the clarity of presentation, we instead consider a toy isotropic MLP with 1 hidden layer and no bias terms as the pretrained backbone:

$$x_{N \times d}^0 \xrightarrow[\omega_{d_{out} \times d_{in}}^1]{\text{Linear}} x_{N \times d}^1 \xrightarrow[\text{e.g., ReLU}]{\text{Act. Func.}} x_{N \times d}^a \xrightarrow[\omega_{d_{out} \times d_{in}}^2]{\text{Linear}} x_{N \times d}^2, \quad (8)$$

where  $x_{N \times d}^0$  represents an input  $N$ -token sequence in the  $d$ -dim space,  $d_{out} = d_{in} = d$  with the subscripts indicating the shape format.

The fine-tuned models via LoRA and our GIFT will respectively be,

$$\text{LoRA: } \begin{bmatrix} \omega^1 \\ \omega^2 \end{bmatrix} + \begin{bmatrix} B^1 \cdot A^1 \\ B^2 \cdot A^2 \end{bmatrix}, \quad \text{GIFT: } \begin{bmatrix} \omega^1 \\ \omega^2 \end{bmatrix} \cdot (\mathbb{I} + \Theta), \quad \Theta \text{ is defined in Eqn. 2,} \quad (9)$$

where if we treat each row in  $\omega^1$  and  $\omega^2$  as  $d_{in}$ -dim parameter-token in the parameter space, LoRA learns separate additive residuals for each of them, while our GIFT shares the same projection/transformation matrix  $\mathbb{I} + \Theta$  for all of them, which is fundamentally different from LoRA and clearly shows fine-tuning a pretrained backbone can be explained via learning a shared transformation matrix. To our knowledge, this perspective of PEFT has not been studied in the prior art. We further show the new formulation of our GIFT leads to two novel aspects in the forward computing and the backward computing respectively.

**i) GIFT Is Exchangeable from the Parameter Space to the Activation Space.** Consider a linear layer with pretrained weights  $\omega \in \mathbb{R}^{d_{out} \times d_{in}}$  and the bias term  $b_{d_{out}}$ , with the proposed two-linear-layer GIFT  $(\phi_{d_{in} \times r}, \psi_{r \times d_{in}})$ , the fine-tuned (GIFTed) weights are,

$$\hat{\omega}_{d_{out} \times d_{in}} = \omega_{d_{out} \times d_{in}} \cdot (\mathbb{I} + \phi_{d_{in} \times r} \cdot \psi_{r \times d_{in}}). \quad (10)$$

We show that *the GIFT can be equivalently applied to the input activation, rather than the pretrained weights, to achieve the same fine-tuning effects*. Let  $x_{N \times d_{in}}$  be the input activation to the linear layer, the output activation is defined by,

$$\hat{y}_{N \times d_{out}} = x_{N \times d_{in}} \cdot \underbrace{\hat{\omega}^\top}_{\text{GIFTed weights}} + b = \underbrace{x_{N \times d_{in}} \cdot (\mathbb{I} + \psi^\top \cdot \phi^\top)}_{\text{GIFTed activation, denoted by } \hat{x}_{N \times d_{in}}} \cdot \omega^\top + b, \quad (11)$$

where we omit some subscripts for clarity, and we can see that the GIFT can be instead applied to the input activation, followed by executing the original pretrained weights. This parameter-activation exchangability is not achievable by LoRA. In practice, we do not apply GIFT to the input activation to be more efficient. We note that although this exchangability holds in general, we do not actually verify it in training due to the computational consideration.

**ii) GIFT Is Global and Top-Down w.r.t. the Gradient Back-Propagation.** During fine-tuning for a downstream task, the derivatives to the learnable parameters  $B$ 's and  $A$ 's in LoRA and those to  $\phi$  and  $\psi$  in our GIFT are also significantly different. Let  $\ell$  be the scalar loss (e.g., the cross-entropy loss) computed at an iteration using one data point for simplicity. For example, in the toy MLP example (Eqn. 8), for  $B^1$  and  $A^1$  in LoRA, we have,

$$\underbrace{\frac{\partial \ell}{\partial B^1}}_{d \times r} = \underbrace{\frac{\partial \ell}{\partial x^1}^\top \cdot x^0}_{d \times N} \cdot \underbrace{A^1^\top}_{N \times d}, \quad \underbrace{\frac{\partial \ell}{\partial A^1}}_{r \times d} = B^1^\top \cdot \underbrace{\frac{\partial \ell}{\partial x^1}^\top \cdot x^0}_{N \times d}. \quad (12)$$

Similarly, for  $\psi$  and  $\phi$  in our GIFT,

$$\frac{\partial \ell}{\partial \psi} = \phi^\top \cdot \underbrace{\omega^1^\top \cdot \frac{\partial \ell}{\partial x^1}^\top \cdot x^0}_{d \times N} + \phi^\top \cdot \underbrace{\omega^2^\top \cdot \frac{\partial \ell}{\partial x^2}^\top \cdot x^a}_{d \times N}, \quad (13)$$

$$\frac{\partial \ell}{\partial \phi} = \underbrace{\omega^1^\top \cdot \frac{\partial \ell}{\partial x^1}^\top \cdot x^0}_{d \times N} \cdot \psi^\top + \underbrace{\omega^2^\top \cdot \frac{\partial \ell}{\partial x^2}^\top \cdot x^a}_{d \times N} \cdot \psi^\top, \quad (14)$$

where  $\psi$  and  $\phi$  gather information from all the layers selected in PEFT since they are shared by them. Furthermore, in terms of the gradient updates,  $\psi$  and  $\phi$  “accumulate” information distilled from data significantly different from, yet more informative than, how  $B$  and  $A$  in LoRA do. At a certain layer, for example  $B^1$  and  $A^1$  “accumulate” gradient modulated input activation (e.g.,  $\frac{\partial \ell}{\partial x^1}^\top \cdot x^0$ 's in Eqn. 12).  $\psi$  and  $\phi$  not only “accumulate” information from all (shared) layers, but also utilize the gradient modulated input activation projected onto the space of the pretrained weights (e.g.,  $\omega^1^\top \cdot \frac{\partial \ell}{\partial x^1}^\top \cdot x^0$  in Eqn. 13 and Eqn. 14). This “top-down” information processing may contribute to the emergent visual interpretability (Sec. 2.5 and Fig. 3).

**GIFT is applicable to Large Models.** The analysis in i) and ii) above hold for for pretrained large isotropic models with a subset of layers  $\{\omega^1, \dots, \omega^i, \dots\}$  selected in PEFT. The simple interpretability of our GIFT remains and the fine-tuned model can be expressed as  $[\dots \omega^1 \dots \omega^i \dots] \cdot [\mathbb{I} \quad \mathbb{I} + \Theta \quad \mathbb{I} \quad \mathbb{I} + \Theta \quad \mathbb{I}]^\top$ , where  $\dots$  represents parameters excluded from fine-tuning.

## 2.5 The Visual Interpretability of Our Two-Linear-Layer Parameterized GIFT

Can we interpret the weight transformation by GIFT in terms of testing data? Let  $C_{d_{out} \times r} = \omega_{d_{out} \times d_{in}} \cdot \phi_{d_{in} \times r}$  be the transformation using the first linear layer of GIFT when it is applied to weights of a pretrained layer. We show that when GIFT is applied to fine-tune the linear projection layers in MHSAs,  $C_{d_{out} \times r}$  can be used as an emergent segmentation/token-clustering head to the output of the projection layer (activation map) to form meaningful segmentation-like clusters in computer vision tasks. With Eqn. 11, we compute  $r$  heatmaps by,

$$\begin{aligned} H_{N \times r} &= \hat{y}_{N \times d_{out}} \cdot C_{d_{out} \times r} \\ &= \hat{x}_{N \times d_{in}} \cdot \omega_{d_{out} \times d_{in}}^\top \cdot \omega_{d_{out} \times d_{in}} \cdot \phi_{d_{in} \times r} + b_{d_{out}} \cdot \omega_{d_{out} \times d_{in}} \cdot \phi_{d_{in} \times r}, \end{aligned} \quad (15)$$

where  $\hat{x}_{N \times d_{in}}$  represents the “GIFTed” activation (Eqn. 11), and the second term is a constant for all testing data. We normalize the  $r$  heatmaps to  $[0, 1]$  individually and use 0.5 as the threshold to generate the visualizations (Figure 3).

## 3 Experiments

We conduct experiments across language and vision tasks by comparing our two-linear-layer parameterized GIFT with various other PEFT methods. We also conduct ablation studies on the different parameterization schemes of GIFT.

Method	Params (%)	Win Rate
[31]GPT-3.5 Turbo 1106	-	86.3
[31]Llama-2 Chat 13B	-	81.1
[31]Llama-2 Chat 7B	-	71.4
Llama-2 7B	[63]Full Finetuning	1.0
	[63]LoRA [19]	0.1245
	RED [63]	0.0039
	DiReFT [64]	0.0039
	LoReFT [64]	0.0039
	GIFT <sub>QV</sub> ( $r = 16$ )	0.0039
	GIFT <sub>QV</sub> ( $r = 128$ )	<b>86.87</b>

Table 1: Results of fine-tuning the pretrained Llama-2 7B [56] with GIFT for **instruction following**. GIFT outperforms prior works with the same parameter budget and even outperforms GPT 3.5 Turbo with an increased budget (which is still 4 times less than LoRA). Unless the source is indicated otherwise by the superscript, the results have been obtained from the respective works.

### 3.1 Instruction Tuning

**Setup:** We use Alpaca-Eval 1.0 [31] to evaluate the performance on GIFT when a language model is finetuned for instruction following. Alpaca-Eval 1.0 measures the win rate against the responses generated by the `text-davinci-003` model using GPT 4 as the annotator. We follow the experimental setup of [64] for all our experiments. We finetune LLaMA-1 7B [55] using the Alpaca52k dataset and evaluate using GPT4 Turbo as the annotator during the hyperparameter search. After finding the best hyperparameters, we finetune Llama-2 7B [56] using the Ultrafeedback dataset [9] and use GPT4 as the annotator with Alpaca-Eval 1.0. This setup prevents overfitting to the hyperparameters and GPT4 as the judge. Our hyperparameter settings can be found in Appendix A.1. We only apply GIFT to the Query+Value layers (denoted by GIFT<sub>QV</sub>) since the evaluation during hyperparameter tuning and final runs requires a paid OpenAI API. Note that [63] and [64] also finetune using the Ultrafeedback dataset.

**Results:** Table 1 shows that given the same parameter budget ( $r = 16$ ), GIFT outperforms prior methods. With an increased budget ( $r = 128$ ), which is still below LoRA, *GIFT even outperforms GPT-3.5 Turbo*. During the hyperparameter tuning, we observe that the win rate does not show significant gains above  $r = 64$ , but we choose  $r = 128$  since it obtains the best results during hyperparameter tuning. These results, along with the observations about the choice of components from the commonsense and arithmetic reasoning, suggest that the performance may improve when other components are finetuned. We leave this study for future work. Examples of raw generations using the finetuned model can be found in Appendix B.

Method		Params (%)	BoolQ	PIQA	SIQA	HellaS.	WinoG.	ARC-e	ARC-c	OBQA	Avg
LLaMA-1	[35]PrefT	0.039	64.3	76.8	73.9	42.1	72.1	72.9	54.0	60.6	64.6
	[35]AdapterS	1.953	63.0	79.2	76.3	67.9	75.7	74.5	57.1	72.4	70.8
	[35]AdapterP	3.542	67.9	76.4	78.8	69.8	78.9	73.7	57.3	75.2	72.3
	[35]LoRA [19]	0.826	68.9	80.7	77.4	78.1	78.8	77.8	61.3	74.8	74.7
	DoRA [35] (Half)	0.427	70.0	82.6	79.7	83.2	80.6	80.6	65.4	77.6	77.5
	DoRA [35]	0.838	68.5	82.9	79.6	84.8	80.8	81.4	65.8	81.0	78.1
	DiReFT [64]	0.031	69.5	83.0	79.0	92.5	80.5	82.2	68.0	77.5	79.0
	LoReFT [64]	0.031	69.3	84.4	80.3	93.1	84.2	83.2	68.2	78.9	80.2
Llama 2	GIFT <sub>QV</sub> ( $r = 64$ )	0.016	69.9	83.2	80.0	93.2	81.7	85.4	70.8	82.5	80.9
	GIFT <sub>Proj</sub> ( $r = 128$ )	0.016	70.1	84.1	80.0	92.9	80.7	84.1	69.2	80.3	80.2
	GIFT <sub>QKVUD</sub> ( $r = 64$ )	0.052	69.7	81.9	79.1	91.6	82.1	82.1	67.2	82.1	79.5
	[35]LoRA [19]	0.826	69.8	79.9	79.5	83.6	82.6	79.8	64.7	81.0	77.6
	DoRA [35] (Half)	0.427	72.0	83.1	79.9	89.1	83.0	84.5	71.0	81.2	80.5
	DoRA [35]	0.838	71.8	83.7	76.0	89.1	82.6	83.7	68.2	82.4	79.7
	DiReFT [64]	0.031	70.8	83.6	80.2	93.6	82.1	84.8	70.4	81.5	80.9
	LoReFT [64]	0.031	71.1	83.8	80.8	94.3	84.5	85.6	72.2	82.3	81.8
Llama 3	GIFT <sub>QV</sub> ( $r = 64$ )	0.016	72.0	84.4	80.9	94.0	85.1	86.9	74.5	82.7	82.6
	GIFT <sub>Proj</sub> ( $r = 128$ )	0.016	72.3	84.6	80.5	93.8	83.9	86.6	74.3	81.6	82.2
	GIFT <sub>QKVUD</sub> ( $r = 64$ )	0.052	71.2	83.7	78.8	92.7	82.9	84.9	69.9	81.5	80.7
	[35]LoRA [19]	0.700	70.8	85.2	79.9	91.7	84.3	84.2	71.2	79.0	80.8
	DoRA [35] (Half)	0.361	74.5	88.8	80.3	95.5	84.7	90.1	79.1	87.2	85.0
	DoRA [35]	0.710	74.6	89.3	79.9	95.5	85.6	90.5	80.4	85.8	85.2
	DiReFT [64]	0.026	73.4	88.7	81.0	95.6	85.5	91.8	81.8	85.4	85.4
	LoReFT [64]	0.026	75.1	90.2	82.0	96.3	87.4	92.4	81.6	87.5	86.6

Table 2: Result comparisons on eight commonsense reasoning benchmarks by fine-tuning the pretrained LLaMA-1 [55] 7B, Llama 2 [56] 7B and Llama 3 8B models. Unless the source is indicated otherwise by the superscript, the results have been obtained from the respective works.

### 3.2 Commonsense Reasoning

**Data:** We test our GIFT for commonsense reasoning by training on a combined training data of eight commonsense reasoning benchmarks (Commonsense170k) following [20] and [64], and evaluate on their test sets individually. Examples in the Commonsense170k are formulated as multiple choice questions and consists of BoolQ [6], PIQA [3], SIQA [51], HellaSwag [67], WinoGrande [50], Arc-e and Arc-c [7], and OBQA [41] datasets.

**Models:** We fine-tune Query and Value layers in the pretrained LLaMA-1 [55], Llama-2 [56] and Llama-3 [1] 8B models using our GIFT. In addition to LoRA, we compare with DoRA [35], a recent variation of LoRA by applying low-rank adaptation in the directional space of pretrained weights, and LoReFT [64] which fine-tunes activation/representation of selected layers and tokens of a pretrained backbone, rather than their pretrained weights. For all our experiments, we replicate the setup of [20] and [64]. We evaluate GIFT applied to various components: (i) Query+Value as proposed in [19], denoted by GIFT<sub>QV</sub> in the table. (ii) Query+Key+Value+Up+Down as proposed in [20, 35], denoted by GIFT<sub>QKVUD</sub> and (iii) final linear Projection layer in the Self-Attention block (Proj) as proposed in [52] and the vision experiments in this paper, denoted by GIFT<sub>Proj</sub>. Details of our hyperparameter tuning and settings can be found in Appendix A.2.

**Results:** As seen in Table 2, our GIFT achieves slightly better accuracy than all the baselines while using significantly less parameters. We note that in contrast to LoReFT which searches over layers and token positions to fine-tune, our GIFT is simply applied to predefined fine-tuning layers such as the query and value layers (GIFT<sub>QV</sub>) following the common practice of LoRA, yet obtains slightly better performance than LoReFT using 2 times less parameters. We also note that applying our GIFT to different components indeed result in different performance on the commonsense reasoning benchmark, e.g., GIFT<sub>QV</sub> and GIFT<sub>Proj</sub> have similar performance, while GIFT<sub>QKVUD</sub> leads to worse performance. Since our GIFT is exchangeable from parameter fine-tuning to activation (representation) fine-tuning (Sec. 2.4), we can further search for layers and token positions when applying GIFT to potentially improve the performance. We leave this direction for future work. Examples of raw generations using the finetuned model can be found in Appendix B.

### 3.3 Arithmetic Reasoning

**Data:** Similar to the commonsense reasoning experiments, we follow [20] and [64], and finetune GIFT on a combined training set of four arithmetic reasoning datasets (Math10k), and evaluate on their individual test sets. The Math10k benchmarks consists of AQuA [34], GSM8k [8], MAWPS

Method	Params (%)	AQuA	GSM8k	MAWPS	SVAMP	Avg
LLaMA-1	[20]PrefT	0.039	14.2	24.4	63.4	38.1
	[20]AdapterS	1.953	15.0	33.3	77.7	52.3
	[20]AdapterP	3.542	18.1	35.3	82.4	49.6
	[20]LoRA [19]	0.826	18.9	37.5	79.0	<b>52.1</b>
	DiReFT [64]	<u>0.031</u>	21.3	24.1	74.5	42.7
	LoReFT [64]	<u>0.031</u>	21.4	26.0	76.2	46.8
	GIFT <sub>QV</sub> ( $r = 64$ )	<b>0.016</b>	21.0	29.7	74.4	48.8
GIFT <sub>Proj</sub> ( $r = 128$ )	<b>0.016</b>	<u>22.6</u>	30.1	76.1	48.8	44.4
	GIFT <sub>QKVUD</sub> ( $r = 64$ )	0.052	<b>24.4</b>	30.7	<b>84.9</b>	47.1
						<b>46.8</b>

Table 3: Comparisons on Arithmetic reasoning benchmarks by fine-tuning the pretrained LLaMA-1 [55] 7B. Unless the source is indicated otherwise by the superscript, the results have been obtained from the respective works.

[25] and SVAMP [44]. While the models are expected to generate a chain-of-thought before the final answer, we only evaluate on the final answer following [64]. We follow the same hyperparameter tuning strategy as that used for commonsense reasoning.

**Models:** Due to computational restrictions and for a fair comparison with prior works, we finetune the LLaMA-1 7B model. As with the commonsense reasoning experiments, we evaluate the effect of applying GIFT to various components (Q+V, Proj and Query+Key+Value+Up+Down).

**Results:** As seen in Table 3, the results with GIFT depend on the component to which it is applied to. When GIFT is applied to Query+Key+Value+Up+Down, GIFT performs equivalent to LoRA. The performance is lower when applied to Query+Value, and in between the two when applied to Proj. Together with the results on the commonsense reasoning benchmark in Table 2, the performance of our GIFT vary with respect to where to apply it and differently across individual benchmarks, which reinforces the need of the search for where to apply fine-tuning as done by LoReFT, which we leave for future work. Examples of raw generations using the finetuned model can be found in Appendix B.

Method	Params (%)	SST-2	MRPC	CoLA	QNLI	RTE	STS-B	Avg.
RoBERTa-Base	[19]FT	100	94.8	90.2	63.6	92.8	78.7	91.2
	[19]BitFit	0.080	93.7	92.7	62.0	91.8	81.5	90.8
	[19]Adpt <sup>D</sup>	0.240	94.2 $\pm$ 0.1	88.5 $\pm$ 1.1	60.8 $\pm$ 0.4	93.1 $\pm$ 0.1	71.5 $\pm$ 2.7	89.7 $\pm$ 0.3
	[19]Adpt <sup>D</sup>	0.720	94.7 $\pm$ 0.3	88.4 $\pm$ 0.1	62.9 $\pm$ 0.9	93.0 $\pm$ 0.2	75.9 $\pm$ 2.2	90.3 $\pm$ 0.1
	[26]LoRA [19]	0.240	95.1 $\pm$ 0.2	89.7 $\pm$ 0.7	63.4 $\pm$ 1.2	93.3 $\pm$ 0.3	86.6 $\pm$ 0.7	91.5 $\pm$ 0.2
	VeRA [26]	<b>0.034</b>	94.6 $\pm$ 0.1	89.5 $\pm$ 0.5	65.6 $\pm$ 0.8	91.8 $\pm$ 0.2	78.7 $\pm$ 0.7	90.7 $\pm$ 0.2
	GIFT <sub>QV</sub> ( $r = 32$ )	0.079	<b>94.8</b> $\pm$ 0.3	<b>90.0</b> $\pm$ 1.1	<b>64.1</b> $\pm$ 1.0	92.7 $\pm$ 0.2	78.7 $\pm$ 2.1	90.3 $\pm$ 0.1
RoBERTa-Large	[19]Adpt <sup>P</sup>	0.847	96.1 $\pm$ 0.3	90.2 $\pm$ 0.7	68.3 $\pm$ 1.0	94.8 $\pm$ 0.2	83.8 $\pm$ 2.9	92.1 $\pm$ 0.7
	[19]Adpt <sup>P</sup>	0.226	96.6 $\pm$ 0.2	89.7 $\pm$ 1.2	67.8 $\pm$ 2.5	94.8 $\pm$ 0.3	80.1 $\pm$ 2.9	91.9 $\pm$ 0.4
	[19]Adpt <sup>H</sup>	1.693	96.2 $\pm$ 0.3	88.7 $\pm$ 2.9	66.5 $\pm$ 4.4	94.7 $\pm$ 0.2	83.4 $\pm$ 1.1	91.0 $\pm$ 1.7
	[19]Adpt <sup>H</sup>	0.226	96.3 $\pm$ 0.5	87.7 $\pm$ 1.7	66.3 $\pm$ 2.0	94.7 $\pm$ 0.2	72.9 $\pm$ 2.9	91.5 $\pm$ 0.5
	[69]LoRA-FA	1.044	96.0	90.0	68.0	94.8	86.1	92.0
	[26]LoRA [19]	0.226	96.2 $\pm$ 0.5	90.2 $\pm$ 1.0	68.2 $\pm$ 1.9	94.8 $\pm$ 0.3	85.2 $\pm$ 1.1	92.3 $\pm$ 0.5
	VeRA [26]	<b>0.017</b>	96.1 $\pm$ 0.1	90.9 $\pm$ 0.7	68.0 $\pm$ 0.8	94.4 $\pm$ 0.2	85.9 $\pm$ 0.7	91.7 $\pm$ 0.8
	GIFT <sub>QV</sub> ( $r = 32$ )	0.037	<b>95.8</b> $\pm$ 1.1	<b>88.7</b> $\pm$ 1.2	<b>67.0</b> $\pm$ 1.5	<b>94.7</b> $\pm$ 0.1	<b>87.0</b> $\pm$ 1.4	<b>91.5</b> $\pm$ 0.8
								<b>87.5</b>

Table 4: Results on the GLUE benchmark. Following the common protocol, we report the Matthew’s Correlation for CoLA, Pearson’s Correlation for STS-B. For all other datasets, we report the accuracy. Unless the source is indicated otherwise by the superscript, the results have been obtained from the respective works.

### 3.4 Language Understanding on GLUE

**Data.** General Language Understanding Evaluation benchmark (GLUE) [61] is a widely used benchmark for sequence classification, where the model must learn to classify the entire sentence into two categories. We finetune RoBERTa-Base/Large models [37] with the pretrained checkpoints from HuggingFace using GIFT. We compare with VeRA [26], which is a recent variant of LoRA. VeRA utilizes randomly initialized and frozen  $A$  and  $B$  (Fig. 1) that are shared across all fine-tuning layers and instead learns scaling coefficients for  $A$  and  $B$ , which significantly reduces the number of learnable parameters. We follow a similar experimental setup as VeRA [26]: We do not evaluate on

Method	Params (%) ↓	GPU Mem (G) ↓	CUBS	Bird	Flower	Dog	Car	Avg
VPT [21]	0.054	2.753	87.88	84.79	98.98	84.51	82.89	87.81
BitFit [66]	0.097	2.673	87.75	84.61	<b>99.32</b>	85.23	84.01	88.18
LoRA [19]	0.172	<b>2.622</b>	88.00	84.94	<b>99.32</b>	85.36	<b>85.92</b>	88.71
GIFT ( $r = 16$ )	<b>0.029</b>	2.646	<b>89.71</b>	<b>86.28</b>	99.22	<b>87.44</b>	84.28	<b>89.39</b>

Table 5: Results on the finegrained visual classification (FGVC) tasks. The number of trainable parameters are reported without the classification head which has the same number of parameters for all the methods. The GPU memory usage is reported via `torch.cuda.max_memory_allocated()` during training with the batch size 32.

Method	Params (%) ↓	GPU Mem (G) ↓	Natural	Specialized	Structured	Avg
VPT [21]	0.054	2.753	81.03	85.65	58.89	72.68
BitFit [66]	0.097	2.673	81.79	85.15	57.75	72.37
LoRA [19]	0.172	<b>2.622</b>	<b>81.96</b>	85.89	60.98	73.95
GIFT ( $r = 16$ )	<b>0.029</b>	2.644	81.95	<b>86.30</b>	<b>61.12</b>	<b>74.09</b>

Table 6: Results on the VTAB-1k benchmark [68]. #Params and GPU Memory are reported in the same way as those in Table 5.

MNLI and QQP tasks due to computational budget restrictions, and hence do not use the MNLI trick as done in LoRA [19]<sup>1</sup>. Our hyperparameters are provided in the Appendix A.4.

**Results.** As seen in Table 4, our GIFT achieves similar performance as prior PEFT methods. We note that although VeRA obtains slightly better performance than our GIFT using less parameters, the randomly initialized and frozen  $A$  and  $B$  seem to be less interpretable. We hypothesize that when a downstream task is out of distribution to the pretraining those randomly initialized  $A$  and  $B$  may have limited expressivity. Those being said, we may harness the VeRA method in our GIFT formulation too, e.g., we may randomly initialize and then frozen  $\phi$  and  $\psi$  in our GIFT and learn the scaling coefficients instead, which we leave for future investigation.

### 3.5 Visual Classification on FGVC and VTAB-1k

**Data.** We evaluate our GIFT on two image classification benchmarks: i) The Visual Task Adaptation Benchmark (VTAB-1k) benchmark [68] consists of 19 tasks in three super-categories (natural, specialized and structured), drawn from a variety of domains, and with various semantics. ii) The fine-grained visual classification (FGVC) benchmark contains 5 datasets – Caltech-UCSD Birds (200 classes) [60], NABirds (555 classes) [17], Oxford Flowers (102 classes) [43], Stanford Cars (196 classes) [14], and Stanford Dogs (120 classes) [23].

We use the ViT-B/16 architecture [12] pretrained on ImageNet21k dataset [10] using a supervised objective. We use the checkpoints from the `timm` package [62]. We compare our GIFT with three baselines: the Visual Prompt Tuning (VPT) [21] method which introduces a predefined number of prompts concatenated with original tokens at each layer (e.g., 5), the BitFit [66] method which fine-tunes all the bias terms in the backbone, and the LoRA [19] method. We leverage the publicly available codes for VPT, BitFit and LoRA, and train them from scratch under the same settings as our GIFT for fair comparisons. We apply LoRA and GIFT to the linear projection layer of the MHSA block. The selection of the linear projection layers in PEFT is based on observations in [52] and verified in our ablation studies (Section 3.6). All hyperparameters are provided in Appendix A.3.

**Results.** Table 5 and Table 6 show that our GIFT performs better than other PEFT methods on both FGVC and VTAB-1k, while using fewer parameters. The GPU memory consumption is similar among the different methods with negligible differences. With 5.9 times less parameters used (0.025M vs 0.147M), on FGVC tasks, our GIFT improves LoRA by 0.68% average Top-1 accuracy. On VTAB-1k tasks, our GIFT slightly outperforms LoRA by 0.14% average Top-1 accuracy. Along with higher performance, our GIFT can form meaningful clusters on the images that localize whole objects as well as object parts, as shown in Figure 3 (and Figure 4 in the Appendix). These localization capabilities could potentially be useful for weakly-supervised object/part segmentation, which we leave for future work.

<sup>1</sup>For experiments with RoBERTa-Base, LoRA [19] use the checkpoints from the MNLI task when fine-tuning on the RTE, STS-B and MRPC tasks.

### 3.6 Ablation Studies

**Different Parameterization Schemas for GIFT.** We evaluate the various schema proposed for GIFT (Section 2.3) on the FGVC benchmark using the same settings as Section 3.5. As seen from Table 7, the simple two-linear layer formulation achieves better or equivalent performance than all other schema at a lower parameter cost. We hypothesize that when a downstream task is out of distribution to the pretraining non-linear relationships between fine-tuning weight-residuals and pretrained weights could be entailed to be helpful, which we also leave for future investigation.

Schema	#Params (M) $\downarrow$	GPU Mem (G) $\downarrow$	CUBS	Bird	Flower	Dog	Car	Avg
Identity	0.025	2.65	<b>89.71</b>	<b>86.28</b>	99.22	<b>87.44</b>	84.28	<b>89.39</b>
Sigmoid	0.025	2.65	89.56	84.61	99.20	86.69	84.04	88.82
GeLU	0.025	2.65	89.70	85.30	99.19	86.71	83.81	88.94
MLP	0.036	2.65	89.06	85.44	<b>99.30</b>	86.17	84.24	88.84
Transformer	0.027	2.65	89.56	86.23	99.24	86.31	84.26	89.12
MLP Mixer	0.125	2.65	88.76	86.21	99.25	86.35	<b>85.66</b>	89.25

Table 7: Comparisons between various parameterization schemas of GIFT on the FGVC benchmark.

**Choice of Fine-Tuning the Projection Layer in MHSAs for Vision Tasks.** As opposed to the common convention of applying PEFT methods to the Query and Value layers, we apply GIFT to the last linear projection layer of the Multi-Head Self Attention block, following [52] who show that the projection layer is a sweet spot to for finetuning and growing model for continual learning. We empirically observe that applying GIFT to the Projection layer has two advantages: (1) it results in better visual clusters (2) achieves almost the same performance as that of the Query and Value layers at half the parameter cost, as seen in Table 8. We also note that in both cases, GIFT performs better than LoRA.

Component	Method	#Params (M) $\downarrow$	GPU Mem (G) $\downarrow$	CUBS	Bird	Flower	Dog	Car	Avg
Proj	LoRA	0.147	2.62	88.00	84.94	<b>99.32</b>	85.36	<b>85.92</b>	88.71
	GIFT	0.025	2.65	<b>89.71</b>	<b>86.28</b>	99.22	<b>87.44</b>	84.28	<b>89.39</b>
Q+V	LoRA	0.295	2.97	87.97	84.85	99.20	84.62	<b>87.03</b>	88.73
	GIFT	0.049	2.97	<b>89.54</b>	<b>86.47</b>	<b>99.45</b>	<b>86.92</b>	85.42	<b>89.56</b>

Table 8: Comparisons between the projection layer in the MHSAs module and the Query+Value layer in PEFT using LoRA and our GIFT on the FGVC benchmark.

## 4 Limitations

In our experiments, we show that for computer vision tasks, semantic meaningful localization capabilities emerge as a by-product in our GIFT. However, it is unclear how exactly they emerge (other than the high-level hypothetical explanations in Sec. 2.4), or how to localize a specific cluster other than manual post-hoc inspection. We also note that the clusters still lack consistency between the “firing patterns” across different instances of the same category (e.g., bird) using the same  $r$ -th head in  $C_{d_{out} \times r}$ . Future research can explore this in detail. It is also unclear if the clusters will form for language models, which we also leave for future work.

## 5 Related Work

**Parameter Efficient Fine-tuning (PEFT).** The goal of PEFT methods is to reduce the computational resources (memory footprint, wall time, etc.) required for fine-tuning large models such as Transformers [57] and Vision Transformers (ViTs) [12]. Prompt-based methods either append prompts to the input tokens [29, 21], or the intermediate layers [30, 36, 71]. Early work on PEFT used sequential/parallel learnable adapters added after the Multi-Head Self Attention and/or FFN blocks [18, 2, 46, 45, 48, 39, 5]. LoRA [19] and its variants [70, 11, 32, 22, 26, 13, 35] learn residuals to the pretrained weight matrices in the form of low-rank factorization, removing the added inference cost in adapter based methods. BitFit [66] fine-tunes all the bias terms in a pretrained backbone.

**Hypernetworks.** Ha *et al.* [15] introduced Hypernetworks, i.e., neural networks that generate the parameters for other neural networks, in language modeling tasks by generating the weights of an LSTM [16]. Hypernetworks have previously been applied for few-shot classification [72, 73], transfer learning [47] and continual learning [59, 65]. Similar to our proposed approach, [47] learns

to adapt a global feature extractor through an adaptation network. In a few shot continual learning setup, [58] uses a hyper-Transformer to generate the parameters for a separate Convolutional Neural Network (ConvNet), which use as inputs both a support set of images of the current task and the ConvNet parameters generated for the previous tasks. HyperFormer++ [40] uses a Multi-Layer Perceptron (MLP) to generate the parameters from layer embedding and a latent vector for Adapters [18] introduced across layers of a pretrained model in a multitask setting. Unlike [40], we directly use the weights of the frozen pretrained model, thus eliminating the need for embeddings.

**Neural Functionals:** Our approach is related to neural functionals that aim to learn deep neural networks acting on the weights of other neural networks. For toy problems, equivariant architectures have been explored for tasks like classifying implicit neural representations [42, 74, 75, 24], adapting model architectures to new domains [42], predicting model generalization performance [74, 75, 24, 33], and learned optimizers [76]. However, our work is the first to explore fine-tuning of a model using its own weights. We do not use equivariant architectures, but note that this direction of work is orthogonal to ours, and future work can explore equivariant architectures for GIFT.

## 6 Conclusion

We present Generative Interpretable Fine-Tuning (GIFT) for parameter-efficient fine-tuning (PEFT) of pretrained Transformer backbones. Our GIFT is a deep weight-residual learning framework which induces explicit relationships between fine-tuning weight-residuals and pretrained weights in a layer-agnostic way. We propose a simple parameterization of the GIFT, consisting of two plain linear layers (without bias term), which leads to linear relationships between the fine-tuning weight-residuals and the pretrained weights in the parameter space, and can be equivalently applied to activations/representations, rendering built-in interpretability of PEFT. Through comprehensive studies on natural language (instruction tuning, commonsense and arithmetic reasoning, and language understanding) and fine-grained visual classification tasks, we show that this simple formulation is highly performant while being more parameter efficient than the baselines, and verify this via ablation studies of a series of non-linear parametrizations. GIFT achieves the best performance among the baselines on instruction following, commonsense reasoning and visual classification, and achieves comparable performance on arithmetic reasoning and language understanding. We further show that when GIFT is applied to fine-tune the projection layers of the Multi-Head Self-Attention blocks for visual tasks, visual interpretability emerges as a by-product.

## Acknowledgements

This research is partly supported by NSF IIS-1909644, ARO Grant W911NF1810295, ARO Grant W911NF2210010, NSF IIS-1822477, NSF CMMI-2024688, NSF IUSE-2013451 and DHHS-ACL Grant 90IFDV0017-01-00. The views and conclusions contained herein are those of the authors and should not be interpreted as necessarily representing the official policies or endorsements, either expressed or implied, of the NSF, ARO, DHHS or the U.S. Government. The U.S. Government is authorized to reproduce and distribute reprints for Governmental purposes notwithstanding any copyright annotation thereon.

## References

- [1] AI@Meta. Llama 3 model card. 2024. URL [https://github.com/meta-llama/llama3/blob/main/MODEL\\_CARD.md](https://github.com/meta-llama/llama3/blob/main/MODEL_CARD.md). 2, 3, 8
- [2] Ankur Bapna and Orhan Firat. Simple, scalable adaptation for neural machine translation. In Kentaro Inui, Jing Jiang, Vincent Ng, and Xiaojun Wan, editors, *Proceedings of the 2019 Conference on Empirical Methods in Natural Language Processing and the 9th International Joint Conference on Natural Language Processing, EMNLP-IJCNLP 2019, Hong Kong, China, November 3-7, 2019*, pages 1538–1548. Association for Computational Linguistics, 2019. doi: 10.18653/V1/D19-1165. URL <https://doi.org/10.18653/v1/D19-1165>. 11
- [3] Yonatan Bisk, Rowan Zellers, Ronan Le Bras, Jianfeng Gao, and Yejin Choi. PIQA: reasoning about physical commonsense in natural language. In *The Thirty-Fourth AAAI Conference on Artificial Intelligence, AAAI 2020, The Thirty-Second Innovative Applications of Artificial Intelligence Conference, IAAI 2020, The Tenth AAAI Symposium on Educational Advances in Artificial Intelligence, EAAI 2020, New York, NY, USA, February 7-12, 2020*, pages 7432–7439.

AAAI Press, 2020. doi: 10.1609/AAAI.V34I05.6239. URL <https://doi.org/10.1609/aaai.v34i05.6239>. 8

[4] Rishi Bommasani, Drew A Hudson, Ehsan Adeli, Russ Altman, Simran Arora, Sydney von Arx, Michael S Bernstein, Jeannette Bohg, Antoine Bosselut, Emma Brunskill, et al. On the opportunities and risks of foundation models. *arXiv preprint arXiv:2108.07258*, 2021. 2

[5] Shoufa Chen, Chongjian Ge, Zhan Tong, Jiangliu Wang, Yibing Song, Jue Wang, and Ping Luo. Adaptformer: Adapting vision transformers for scalable visual recognition. In *NeurIPS*, 2022. URL [http://papers.nips.cc/paper\\_files/paper/2022/hash/69e2f49ab0837b71b0e0cb7c555990f8-Abstract-Conference.html](http://papers.nips.cc/paper_files/paper/2022/hash/69e2f49ab0837b71b0e0cb7c555990f8-Abstract-Conference.html). 11

[6] Christopher Clark, Kenton Lee, Ming-Wei Chang, Tom Kwiatkowski, Michael Collins, and Kristina Toutanova. Boolq: Exploring the surprising difficulty of natural yes/no questions. In Jill Burstein, Christy Doran, and Thamar Solorio, editors, *Proceedings of the 2019 Conference of the North American Chapter of the Association for Computational Linguistics: Human Language Technologies, NAACL-HLT 2019, Minneapolis, MN, USA, June 2-7, 2019, Volume 1 (Long and Short Papers)*, pages 2924–2936. Association for Computational Linguistics, 2019. doi: 10.18653/V1/N19-1300. URL <https://doi.org/10.18653/v1/n19-1300>. 8

[7] Peter Clark, Isaac Cowhey, Oren Etzioni, Tushar Khot, Ashish Sabharwal, Carissa Schoenick, and Oyvind Tafjord. Think you have solved question answering? try arc, the AI2 reasoning challenge. *CoRR*, abs/1803.05457, 2018. URL <http://arxiv.org/abs/1803.05457>. 8

[8] Karl Cobbe, Vineet Kosaraju, Mohammad Bavarian, Mark Chen, Heewoo Jun, Lukasz Kaiser, Matthias Plappert, Jerry Tworek, Jacob Hilton, Reiichiro Nakano, Christopher Hesse, and John Schulman. Training verifiers to solve math word problems. *CoRR*, abs/2110.14168, 2021. URL <https://arxiv.org/abs/2110.14168>. 8, 20

[9] Ganqu Cui, Lifan Yuan, Ning Ding, Guanming Yao, Wei Zhu, Yuan Ni, Guotong Xie, Zhiyuan Liu, and Maosong Sun. Ultrafeedback: Boosting language models with high-quality feedback. *CoRR*, abs/2310.01377, 2023. doi: 10.48550/ARXIV.2310.01377. URL <https://doi.org/10.48550/arXiv.2310.01377>. 7, 20

[10] Jia Deng, Wei Dong, Richard Socher, Li-Jia Li, Kai Li, and Li Fei-Fei. Imagenet: A large-scale hierarchical image database. In *2009 IEEE Computer Society Conference on Computer Vision and Pattern Recognition (CVPR 2009), 20-25 June 2009, Miami, Florida, USA*, pages 248–255. IEEE Computer Society, 2009. doi: 10.1109/CVPR.2009.5206848. URL <https://doi.org/10.1109/CVPR.2009.5206848>. 10, 21

[11] Tim Dettmers, Artidoro Pagnoni, Ari Holtzman, and Luke Zettlemoyer. Qlora: Efficient finetuning of quantized llms. *CoRR*, abs/2305.14314, 2023. doi: 10.48550/ARXIV.2305.14314. URL <https://doi.org/10.48550/arXiv.2305.14314>. 2, 11

[12] Alexey Dosovitskiy, Lucas Beyer, Alexander Kolesnikov, Dirk Weissenborn, Xiaohua Zhai, Thomas Unterthiner, Mostafa Dehghani, Matthias Minderer, Georg Heigold, Sylvain Gelly, Jakob Uszkoreit, and Neil Houlsby. An image is worth 16x16 words: Transformers for image recognition at scale. In *9th International Conference on Learning Representations, ICLR 2021, Virtual Event, Austria, May 3-7, 2021*. OpenReview.net, 2021. URL <https://openreview.net/forum?id=YicbFdNTTy>. 2, 4, 5, 10, 11, 21

[13] Ziqi Gao, Qichao Wang, Aochuan Chen, Zijing Liu, Bingzhe Wu, Liang Chen, and Jia Li. Parameter-efficient fine-tuning with discrete fourier transform. *arXiv preprint arXiv:2405.03003*, 2024. 2, 11

[14] Timnit Gebru, Jonathan Krause, Yilun Wang, Duyun Chen, Jia Deng, and Li Fei-Fei. Fine-grained car detection for visual census estimation. In Satinder Singh and Shaul Markovitch, editors, *Proceedings of the Thirty-First AAAI Conference on Artificial Intelligence, February 4-9, 2017, San Francisco, California, USA*, pages 4502–4508. AAAI Press, 2017. doi: 10.1609/AAAI.V31I1.11174. URL <https://doi.org/10.1609/aaai.v31i1.11174>. 10, 21

[15] David Ha, Andrew M. Dai, and Quoc V. Le. HyperNetworks. In *International Conference on Learning Representations*, October 2016. URL <https://openreview.net/forum?id=rkpACe1lx>. 11

[16] Sepp Hochreiter and Jürgen Schmidhuber. Long short-term memory. *Neural Comput.*, 9(8):1735–1780, nov 1997. ISSN 0899-7667. doi: 10.1162/neco.1997.9.8.1735. URL <https://doi.org/10.1162/neco.1997.9.8.1735>. 11

[17] Grant Van Horn, Steve Branson, Ryan Farrell, Scott Haber, Jessie Barry, Panos Ipeirotis, Pietro Perona, and Serge J. Belongie. Building a bird recognition app and large scale dataset with citizen scientists: The fine print in fine-grained dataset collection. In *IEEE Conference on Computer Vision and Pattern Recognition, CVPR 2015, Boston, MA, USA, June 7-12, 2015*, pages 595–604. IEEE Computer Society, 2015. doi: 10.1109/CVPR.2015.7298658. URL <https://doi.org/10.1109/CVPR.2015.7298658>. 4, 10

[18] Neil Houlsby, Andrei Giurgiu, Stanislaw Jastrzebski, Bruna Morrone, Quentin de Laroussilhe, Andrea Gesmundo, Mona Attariyan, and Sylvain Gelly. Parameter-efficient transfer learning for NLP. In Kamalika Chaudhuri and Ruslan Salakhutdinov, editors, *Proceedings of the 36th International Conference on Machine Learning, ICML 2019, 9-15 June 2019, Long Beach, California, USA*, volume 97 of *Proceedings of Machine Learning Research*, pages 2790–2799. PMLR, 2019. URL <http://proceedings.mlr.press/v97/houlsby19a.html>. 11, 12

[19] Edward J Hu, yelong shen, Phillip Wallis, Zeyuan Allen-Zhu, Yuanzhi Li, Shean Wang, Lu Wang, and Weizhu Chen. LoRA: Low-rank adaptation of large language models. In *International Conference on Learning Representations*, 2022. URL <https://openreview.net/forum?id=nZeVKeeFYf9>. 2, 3, 4, 7, 8, 9, 10, 11, 21

[20] Zhiqiang Hu, Lei Wang, Yihuai Lan, Wanyu Xu, Ee-Peng Lim, Lidong Bing, Xing Xu, Soujanya Poria, and Roy Ka-Wei Lee. Llm-adapters: An adapter family for parameter-efficient fine-tuning of large language models. In Houda Bouamor, Juan Pino, and Kalika Bali, editors, *Proceedings of the 2023 Conference on Empirical Methods in Natural Language Processing, EMNLP 2023, Singapore, December 6-10, 2023*, pages 5254–5276. Association for Computational Linguistics, 2023. doi: 10.18653/V1/2023.EMNLP-MAIN.319. URL <https://doi.org/10.18653/v1/2023.emnlp-main.319>. 8, 9

[21] Menglin Jia, Luming Tang, Bor-Chun Chen, Claire Cardie, Serge J. Belongie, Bharath Hariharan, and Ser-Nam Lim. Visual prompt tuning. In Shai Avidan, Gabriel J. Brostow, Moustapha Cissé, Giovanni Maria Farinella, and Tal Hassner, editors, *Computer Vision - ECCV 2022 - 17th European Conference, Tel Aviv, Israel, October 23-27, 2022, Proceedings, Part XXXIII*, volume 13693 of *Lecture Notes in Computer Science*, pages 709–727. Springer, 2022. doi: 10.1007/978-3-031-19827-4\_41. URL [https://doi.org/10.1007/978-3-031-19827-4\\_41](https://doi.org/10.1007/978-3-031-19827-4_41). 4, 10, 11

[22] Shibo Jie and Zhi-Hong Deng. Fact: Factor-tuning for lightweight adaptation on vision transformer. In Brian Williams, Yiling Chen, and Jennifer Neville, editors, *Thirty-Seventh AAAI Conference on Artificial Intelligence, AAAI 2023, Thirty-Fifth Conference on Innovative Applications of Artificial Intelligence, IAAI 2023, Thirteenth Symposium on Educational Advances in Artificial Intelligence, EAAI 2023, Washington, DC, USA, February 7-14, 2023*, pages 1060–1068. AAAI Press, 2023. doi: 10.1609/AAAI.V37I1.25187. URL <https://doi.org/10.1609/aaai.v37i1.25187>. 2, 11

[23] Aditya Khosla, Nityananda Jayadevaprakash, Bangpeng Yao, and Li Fei-Fei. Novel dataset for fine-grained image categorization. In *First Workshop on Fine-Grained Visual Categorization, IEEE Conference on Computer Vision and Pattern Recognition*, Colorado Springs, CO, June 2011. 10

[24] Miltiadis Kofinas, Boris Knyazev, Yan Zhang, Yunlu Chen, Gertjan J. Burghouts, Efstratios Gavves, Cees G. M. Snoek, and David W. Zhang. Graph neural networks for learning equivariant representations of neural networks. *CoRR*, abs/2403.12143, 2024. doi: 10.48550/ARXIV.2403.12143. URL <https://doi.org/10.48550/arXiv.2403.12143>. 12

[25] Rik Koncel-Kedziorski, Subhro Roy, Aida Amini, Nate Kushman, and Hannaneh Hajishirzi. MAWPS: A math word problem repository. In Kevin Knight, Ani Nenkova, and Owen Rambow, editors, *NAACL HLT 2016, The 2016 Conference of the North American Chapter of the Association for Computational Linguistics: Human Language Technologies, San Diego California, USA, June 12-17, 2016*, pages 1152–1157. The Association for Computational Linguistics, 2016. doi: 10.18653/V1/N16-1136. URL <https://doi.org/10.18653/v1/n16-1136>. 9

[26] Dawid Jan Kopiczko, Tijmen Blankevoort, and Yuki Markus Asano. Vera: Vector-based random matrix adaptation. *CoRR*, abs/2310.11454, 2023. doi: 10.48550/ARXIV.2310.11454. URL <https://doi.org/10.48550/arXiv.2310.11454>. 2, 9, 11, 21, 22

[27] Alex Krizhevsky, Ilya Sutskever, and Geoffrey E Hinton. Imagenet classification with deep convolutional neural networks. In F. Pereira, C.J. Burges, L. Bottou, and K.Q. Weinberger, editors, *Advances in Neural Information Processing Systems*, volume 25. Curran Associates, Inc., 2012. URL [https://proceedings.neurips.cc/paper\\_files/paper/2012/file/c399862d3b9d6b76c8436e924a68c45b-Paper.pdf](https://proceedings.neurips.cc/paper_files/paper/2012/file/c399862d3b9d6b76c8436e924a68c45b-Paper.pdf). 1

[28] Yoonho Lee, Annie S Chen, Fahim Tajwar, Ananya Kumar, Huaxiu Yao, Percy Liang, and Chelsea Finn. Surgical fine-tuning improves adaptation to distribution shifts. *arXiv preprint arXiv:2210.11466*, 2022. 2

[29] Brian Lester, Rami Al-Rfou, and Noah Constant. The power of scale for parameter-efficient prompt tuning. In Marie-Francine Moens, Xuanjing Huang, Lucia Specia, and Scott Wen-tau Yih, editors, *Proceedings of the 2021 Conference on Empirical Methods in Natural Language Processing, EMNLP 2021, Virtual Event / Punta Cana, Dominican Republic, 7-11 November, 2021*, pages 3045–3059. Association for Computational Linguistics, 2021. doi: 10.18653/V1/2021.EMNLP-MAIN.243. URL <https://doi.org/10.18653/v1/2021.emnlp-main.243>. 11

[30] Xiang Lisa Li and Percy Liang. Prefix-tuning: Optimizing continuous prompts for generation. In Chengqing Zong, Fei Xia, Wenjie Li, and Roberto Navigli, editors, *Proceedings of the 59th Annual Meeting of the Association for Computational Linguistics and the 11th International Joint Conference on Natural Language Processing, ACL/IJCNLP 2021, (Volume 1: Long Papers), Virtual Event, August 1-6, 2021*, pages 4582–4597. Association for Computational Linguistics, 2021. doi: 10.18653/V1/2021.ACL-LONG.353. URL <https://doi.org/10.18653/v1/2021.acl-long.353>. 11

[31] Xuechen Li, Tianyi Zhang, Yann Dubois, Rohan Taori, Ishaan Gulrajani, Carlos Guestrin, Percy Liang, and Tatsunori B. Hashimoto. Alpacaeval: An automatic evaluator of instruction-following models. [https://github.com/tatsu-lab/alpaca\\_eval](https://github.com/tatsu-lab/alpaca_eval), 2023. 3, 7, 20

[32] Vladislav Lialin, Namrata Shivagunde, Sherin Muckatira, and Anna Rumshisky. Stack more layers differently: High-rank training through low-rank updates. *CoRR*, abs/2307.05695, 2023. doi: 10.48550/ARXIV.2307.05695. URL <https://doi.org/10.48550/arXiv.2307.05695>. 2, 11

[33] Derek Lim, Haggai Maron, Marc T. Law, Jonathan Lorraine, and James Lucas. Graph metanetworks for processing diverse neural architectures. *CoRR*, abs/2312.04501, 2023. doi: 10.48550/ARXIV.2312.04501. URL <https://doi.org/10.48550/arXiv.2312.04501>. 12

[34] Wang Ling, Dani Yogatama, Chris Dyer, and Phil Blunsom. Program induction by rationale generation: Learning to solve and explain algebraic word problems. In Regina Barzilay and Min-Yen Kan, editors, *Proceedings of the 55th Annual Meeting of the Association for Computational Linguistics, ACL 2017, Vancouver, Canada, July 30 - August 4, Volume 1: Long Papers*, pages 158–167. Association for Computational Linguistics, 2017. doi: 10.18653/V1/P17-1015. URL <https://doi.org/10.18653/v1/P17-1015>. 8

[35] Shih-Yang Liu, Chien-Yi Wang, Hongxu Yin, Pavlo Molchanov, Yu-Chiang Frank Wang, Kwang-Ting Cheng, and Min-Hung Chen. Dora: Weight-decomposed low-rank adaptation. *CoRR*, abs/2402.09353, 2024. doi: 10.48550/ARXIV.2402.09353. URL <https://doi.org/10.48550/arXiv.2402.09353>. 2, 3, 8, 11

[36] Xiao Liu, Kaixuan Ji, Yicheng Fu, Zhengxiao Du, Zhilin Yang, and Jie Tang. P-tuning v2: Prompt tuning can be comparable to fine-tuning universally across scales and tasks. *CoRR*, abs/2110.07602, 2021. URL <https://arxiv.org/abs/2110.07602>. 11

[37] Yinhan Liu, Myle Ott, Naman Goyal, Jingfei Du, Mandar Joshi, Danqi Chen, Omer Levy, Mike Lewis, Luke Zettlemoyer, and Veselin Stoyanov. Roberta: A robustly optimized BERT pretraining approach. *CoRR*, abs/1907.11692, 2019. URL <http://arxiv.org/abs/1907.11692>. 9, 21

[38] Ilya Loshchilov and Frank Hutter. Decoupled weight decay regularization. In *7th International Conference on Learning Representations, ICLR 2019, New Orleans, LA, USA, May 6-9, 2019*. OpenReview.net, 2019. URL <https://openreview.net/forum?id=Bkg6RiCqY7>. 21

[39] Rabeeh Karimi Mahabadi, James Henderson, and Sebastian Ruder. Compacter: Efficient low-rank hypercomplex adapter layers. In Marc'Aurelio Ranzato, Alina Beygelzimer, Yann N. Dauphin, Percy Liang, and Jennifer Wortman Vaughan, editors, *Advances in Neural Information Processing Systems 34: Annual Conference on Neural Information Processing Systems 2021, NeurIPS 2021, December 6-14, 2021, virtual*, pages 1022–1035, 2021. URL <https://proceedings.neurips.cc/paper/2021/hash/081be9fdff07f3bc808f935906ef70c0-Abstract.html>. 11

[40] Rabeeh Karimi Mahabadi, Sebastian Ruder, Mostafa Dehghani, and James Henderson. Parameter-efficient multi-task fine-tuning for transformers via shared hypernetworks. In Chengqing Zong, Fei Xia, Wenjie Li, and Roberto Navigli, editors, *Proceedings of the 59th Annual Meeting of the Association for Computational Linguistics and the 11th International Joint Conference on Natural Language Processing, ACL/IJCNLP 2021, (Volume 1: Long Papers), Virtual Event, August 1-6, 2021*, pages 565–576. Association for Computational Linguistics, 2021. doi: 10.18653/V1/2021.ACL-LONG.47. URL <https://doi.org/10.18653/v1/2021.acl-long.47>. 12

[41] Todor Mihaylov, Peter Clark, Tushar Khot, and Ashish Sabharwal. Can a suit of armor conduct electricity? A new dataset for open book question answering. In Ellen Riloff, David Chiang, Julia Hockenmaier, and Jun’ichi Tsujii, editors, *Proceedings of the 2018 Conference on Empirical Methods in Natural Language Processing, Brussels, Belgium, October 31 - November 4, 2018*, pages 2381–2391. Association for Computational Linguistics, 2018. doi: 10.18653/V1/D18-1260. URL <https://doi.org/10.18653/v1/d18-1260>. 8

[42] Aviv Navon, Aviv Shamsian, Idan Achituv, Ethan Fetaya, Gal Chechik, and Haggai Maron. Equivariant architectures for learning in deep weight spaces. In Andreas Krause, Emma Brunskill, Kyunghyun Cho, Barbara Engelhardt, Sivan Sabato, and Jonathan Scarlett, editors, *International Conference on Machine Learning, ICML 2023, 23-29 July 2023, Honolulu, Hawaii, USA*, volume 202 of *Proceedings of Machine Learning Research*, pages 25790–25816. PMLR, 2023. URL <https://proceedings.mlr.press/v202/navon23a.html>. 12

[43] Maria-Elena Nilsback and Andrew Zisserman. Automated flower classification over a large number of classes. In *Sixth Indian Conference on Computer Vision, Graphics & Image Processing, ICVGIP 2008, Bhubaneswar, India, 16-19 December 2008*, pages 722–729. IEEE Computer Society, 2008. doi: 10.1109/ICVGIP.2008.47. URL <https://doi.org/10.1109/ICVGIP.2008.47>. 10

[44] Arkil Patel, Satwik Bhattacharya, and Navin Goyal. Are NLP models really able to solve simple math word problems? In Kristina Toutanova, Anna Rumshisky, Luke Zettlemoyer, Dilek Hakkani-Tür, Iz Beltagy, Steven Bethard, Ryan Cotterell, Tanmoy Chakraborty, and Yichao Zhou, editors, *Proceedings of the 2021 Conference of the North American Chapter of the Association for Computational Linguistics: Human Language Technologies, NAACL-HLT 2021, Online, June 6-11, 2021*, pages 2080–2094. Association for Computational Linguistics, 2021. doi: 10.18653/V1/2021.NAACL-MAIN.168. URL <https://doi.org/10.18653/v1/2021.naacl-main.168>. 9

[45] Jonas Pfeiffer, Ivan Vulic, Iryna Gurevych, and Sebastian Ruder. MAD-X: an adapter-based framework for multi-task cross-lingual transfer. In Bonnie Webber, Trevor Cohn, Yulan He, and Yang Liu, editors, *Proceedings of the 2020 Conference on Empirical Methods in Natural Language Processing, EMNLP 2020, Online, November 16-20, 2020*, pages 7654–7673. Association for Computational Linguistics, 2020. doi: 10.18653/V1/2020.EMNLP-MAIN.617. URL <https://doi.org/10.18653/v1/2020.emnlp-main.617>. 11

[46] Jonas Pfeiffer, Aishwarya Kamath, Andreas Rücklé, Kyunghyun Cho, and Iryna Gurevych. Adapterfusion: Non-destructive task composition for transfer learning. In Paola Merlo, Jörg Tiedemann, and Reut Tsarfaty, editors, *Proceedings of the 16th Conference of the European Chapter of the Association for Computational Linguistics: Main Volume, EACL 2021, Online, April 19 - 23, 2021*, pages 487–503. Association for Computational Linguistics, 2021.

doi: 10.18653/V1/2021.EACL-MAIN.39. URL <https://doi.org/10.18653/v1/2021.eacl-main.39>. 11

- [47] James Requeima, Jonathan Gordon, John Bronskill, Sebastian Nowozin, and Richard E Turner. Fast and Flexible Multi-Task Classification using Conditional Neural Adaptive Processes. In *Advances in Neural Information Processing Systems*, volume 32. Curran Associates, Inc., 2019. URL [https://proceedings.neurips.cc/paper\\_files/paper/2019/hash/1138d90ef0a0848a542e57d1595f58ea-Abstract.html](https://proceedings.neurips.cc/paper_files/paper/2019/hash/1138d90ef0a0848a542e57d1595f58ea-Abstract.html). 11
- [48] Andreas Rücklé, Gregor Geigle, Max Glockner, Tilman Beck, Jonas Pfeiffer, Nils Reimers, and Iryna Gurevych. Adapterdrop: On the efficiency of adapters in transformers. In Marie-Francine Moens, Xuanjing Huang, Lucia Specia, and Scott Wen-tau Yih, editors, *Proceedings of the 2021 Conference on Empirical Methods in Natural Language Processing, EMNLP 2021, Virtual Event / Punta Cana, Dominican Republic, 7-11 November, 2021*, pages 7930–7946. Association for Computational Linguistics, 2021. doi: 10.18653/V1/2021.EMNLP-MAIN.626. URL <https://doi.org/10.18653/v1/2021.emnlp-main.626>. 11
- [49] Olga Russakovsky, Jia Deng, Hao Su, Jonathan Krause, Sanjeev Satheesh, Sean Ma, Zhiheng Huang, Andrej Karpathy, Aditya Khosla, Michael Bernstein, Alexander C. Berg, and Li Fei-Fei. ImageNet Large Scale Visual Recognition Challenge. *International Journal of Computer Vision (IJCV)*, 115(3):211–252, 2015. doi: 10.1007/s11263-015-0816-y. 1, 4
- [50] Keisuke Sakaguchi, Ronan Le Bras, Chandra Bhagavatula, and Yejin Choi. Winogrande: an adversarial winograd schema challenge at scale. *Commun. ACM*, 64(9):99–106, 2021. doi: 10.1145/3474381. URL <https://doi.org/10.1145/3474381>. 8
- [51] Maarten Sap, Hannah Rashkin, Derek Chen, Ronan Le Bras, and Yejin Choi. Socialqa: Commonsense reasoning about social interactions. *CoRR*, abs/1904.09728, 2019. URL <http://arxiv.org/abs/1904.09728>. 8
- [52] Chinmay Savadikar, Michelle Dai, and Tianfu Wu. Learning to grow artificial hippocampi in vision transformers for resilient lifelong learning. *arXiv preprint arXiv:2303.08250*, 2023. 8, 10, 11
- [53] Baifeng Shi, Siyu Gai, Trevor Darrell, and Xin Wang. Refocusing is key to transfer learning. *arXiv preprint arXiv:2305.15542*, 2023. 21
- [54] Ilya O Tolstikhin, Neil Houlsby, Alexander Kolesnikov, Lucas Beyer, Xiaohua Zhai, Thomas Unterthiner, Jessica Yung, Andreas Steiner, Daniel Keysers, Jakob Uszkoreit, et al. Mlp-mixer: An all-mlp architecture for vision. *Advances in neural information processing systems*, 34: 24261–24272, 2021. 5
- [55] Hugo Touvron, Thibaut Lavril, Gautier Izacard, Xavier Martinet, Marie-Anne Lachaux, Timothée Lacroix, Baptiste Rozière, Naman Goyal, Eric Hambro, Faisal Azhar, Aurélien Rodriguez, Armand Joulin, Édouard Grave, and Guillaume Lample. Llama: Open and efficient foundation language models. *CoRR*, abs/2302.13971, 2023. doi: 10.48550/ARXIV.2302.13971. URL <https://doi.org/10.48550/arXiv.2302.13971>. 2, 3, 7, 8, 9, 20
- [56] Hugo Touvron, Louis Martin, Kevin Stone, Peter Albert, Amjad Almahairi, Yasmine Babaei, Nikolay Bashlykov, Soumya Batra, Prajjwal Bhargava, Shruti Bhosale, Dan Bikel, Lukas Blecher, Cristian Canton-Ferrer, Moya Chen, Guillem Cucurull, David Esiobu, Jude Fernandes, Jeremy Fu, Wenyin Fu, Brian Fuller, Cynthia Gao, Vedanuj Goswami, Naman Goyal, Anthony Hartshorn, Saghar Hosseini, Rui Hou, Hakan Inan, Marcin Kardas, Viktor Kerkez, Madian Khabsa, Isabel Kloumann, Artem Korenev, Punit Singh Koura, Marie-Anne Lachaux, Thibaut Lavril, Jenya Lee, Diana Liskovich, Yinghai Lu, Yuning Mao, Xavier Martinet, Todor Mihaylov, Pushkar Mishra, Igor Molybog, Yixin Nie, Andrew Poulton, Jeremy Reizenstein, Rashi Rungra, Kalyan Saladi, Alan Schelten, Ruan Silva, Eric Michael Smith, Ranjan Subramanian, Xiaoqing Ellen Tan, Binh Tang, Ross Taylor, Adina Williams, Jian Xiang Kuan, Puxin Xu, Zheng Yan, Iliyan Zarov, Yuchen Zhang, Angela Fan, Melanie Kambadur, Sharan Narang, Aurélien Rodriguez, Robert Stojnic, Sergey Edunov, and Thomas Scialom. Llama 2: Open foundation and fine-tuned chat models. *CoRR*, abs/2307.09288, 2023. doi: 10.48550/ARXIV.2307.09288. URL <https://doi.org/10.48550/arXiv.2307.09288>. 2, 3, 4, 7, 8, 20

[57] Ashish Vaswani, Noam Shazeer, Niki Parmar, Jakob Uszkoreit, Llion Jones, Aidan N. Gomez, Łukasz Kaiser, and Illia Polosukhin. Attention is all you need. In Isabelle Guyon, Ulrike von Luxburg, Samy Bengio, Hanna M. Wallach, Rob Fergus, S. V. N. Vishwanathan, and Roman Garnett, editors, *Advances in Neural Information Processing Systems 30: Annual Conference on Neural Information Processing Systems 2017, December 4-9, 2017, Long Beach, CA, USA*, pages 5998–6008, 2017. URL <https://proceedings.neurips.cc/paper/2017/hash/3f5ee243547dee91fb053c1c4a845aa-Abstract.html>. 2, 5, 11

[58] Max Vladymyrov, Andrey Zhmoginov, and Mark Sandler. Continual few-shot learning using hypertransformers. *arXiv preprint arXiv:2301.04584*, 2023. 12

[59] Johannes von Oswald, Christian Henning, Benjamin F. Grewe, and João Sacramento. Continual learning with hypernetworks. In *International Conference on Learning Representations*, 2020. URL <https://openreview.net/forum?id=SJgwNerKvB>. 11

[60] Catherine Wah, Steve Branson, Peter Welinder, Pietro Perona, and Serge Belongie. *The Caltech-UCSD Birds-200-2011 Dataset*. Jul 2011. 10

[61] Alex Wang, Amanpreet Singh, Julian Michael, Felix Hill, Omer Levy, and Samuel R. Bowman. GLUE: A multi-task benchmark and analysis platform for natural language understanding. In Tal Linzen, Grzegorz Chrupala, and Afra Alishahi, editors, *Proceedings of the Workshop: Analyzing and Interpreting Neural Networks for NLP, BlackboxNLP@EMNLP 2018, Brussels, Belgium, November 1, 2018*, pages 353–355. Association for Computational Linguistics, 2018. doi: 10.18653/V1/W18-5446. URL <https://doi.org/10.18653/v1/w18-5446>. 9

[62] Ross Wightman. Pytorch image models. <https://github.com/rwightman/pytorch-image-models>, 2019. 10

[63] Muling Wu, Wenhao Liu, Xiaohua Wang, Tianlong Li, Changze Lv, Zixuan Ling, Jianhao Zhu, Cenyuan Zhang, Xiaoqing Zheng, and Xuanjing Huang. Advancing parameter efficiency in fine-tuning via representation editing. *CoRR*, abs/2402.15179, 2024. doi: 10.48550/ARXIV.2402.15179. URL <https://doi.org/10.48550/arXiv.2402.15179>. 3, 7

[64] Zhengxuan Wu, Aryaman Arora, Zheng Wang, Atticus Geiger, Dan Jurafsky, Christopher D. Manning, and Christopher Potts. Reft: Representation finetuning for language models. *CoRR*, abs/2404.03592, 2024. doi: 10.48550/ARXIV.2404.03592. URL <https://doi.org/10.48550/arXiv.2404.03592>. 3, 7, 8, 9, 20

[65] Li Yin, Juan M. Perez-Rua, and Kevin J. Liang. Sylph: A hypernetwork framework for incremental few-shot object detection. In *IEEE/CVF Conference on Computer Vision and Pattern Recognition, CVPR 2022, New Orleans, LA, USA, June 18-24, 2022*, pages 9025–9035. IEEE, 2022. doi: 10.1109/CVPR52688.2022.00883. URL <https://doi.org/10.1109/CVPR52688.2022.00883>. 11

[66] Elad Ben Zaken, Yoav Goldberg, and Shauli Ravfogel. Bitfit: Simple parameter-efficient fine-tuning for transformer-based masked language-models. In *Proceedings of the 60th Annual Meeting of the Association for Computational Linguistics (Volume 2: Short Papers)*, pages 1–9, 2022. 4, 10, 11

[67] Rowan Zellers, Ari Holtzman, Yonatan Bisk, Ali Farhadi, and Yejin Choi. Hellaswag: Can a machine really finish your sentence? In Anna Korhonen, David R. Traum, and Lluís Márquez, editors, *Proceedings of the 57th Conference of the Association for Computational Linguistics, ACL 2019, Florence, Italy, July 28- August 2, 2019, Volume 1: Long Papers*, pages 4791–4800. Association for Computational Linguistics, 2019. doi: 10.18653/V1/P19-1472. URL <https://doi.org/10.18653/v1/p19-1472>. 8

[68] Xiaohua Zhai, Joan Puigcerver, Alexander Kolesnikov, Pierre Ruyssen, Carlos Riquelme, Mario Lucic, Josip Djolonga, André Susano Pinto, Maxim Neumann, Alexey Dosovitskiy, Lucas Beyer, Olivier Bachem, Michael Tschannen, Marcin Michalski, Olivier Bousquet, Sylvain Gelly, and Neil Houlsby. The visual task adaptation benchmark. *CoRR*, abs/1910.04867, 2019. URL <http://arxiv.org/abs/1910.04867>. 10, 21

[69] Longteng Zhang, Lin Zhang, Shaohuai Shi, Xiaowen Chu, and Bo Li. Lora-fa: Memory-efficient low-rank adaptation for large language models fine-tuning. *CoRR*, abs/2308.03303, 2023. doi: 10.48550/ARXIV.2308.03303. URL <https://doi.org/10.48550/arXiv.2308.03303>. 9

[70] Qingru Zhang, Minshuo Chen, Alexander Bukharin, Pengcheng He, Yu Cheng, Weizhu Chen, and Tuo Zhao. Adaptive budget allocation for parameter-efficient fine-tuning. In *The Eleventh International Conference on Learning Representations, ICLR 2023, Kigali, Rwanda, May 1-5, 2023*. OpenReview.net, 2023. URL <https://openreview.net/pdf?id=lq62uWRJjiY>. 2, 11

[71] Renrui Zhang, Jiaming Han, Aojun Zhou, Xiangfei Hu, Shilin Yan, Pan Lu, Hongsheng Li, Peng Gao, and Yu Qiao. Llama-adapter: Efficient fine-tuning of language models with zero-init attention. *CoRR*, abs/2303.16199, 2023. doi: 10.48550/ARXIV.2303.16199. URL <https://doi.org/10.48550/arXiv.2303.16199>. 11

[72] Dominic Zhao, Seijin Kobayashi, João Sacramento, and Johannes von Oswald. Meta-learning via hypernetworks. In *4th Workshop on Meta-Learning at NeurIPS 2020 (MetaLearn 2020)*. NeurIPS, 2020. 11

[73] Andrey Zhmoginov, Mark Sandler, and Maksym Vladymyrov. HyperTransformer: Model generation for supervised and semi-supervised few-shot learning. In Kamalika Chaudhuri, Stefanie Jegelka, Le Song, Csaba Szepesvari, Gang Niu, and Sivan Sabato, editors, *Proceedings of the 39th International Conference on Machine Learning*, volume 162 of *Proceedings of Machine Learning Research*, pages 27075–27098. PMLR, 17–23 Jul 2022. URL <https://proceedings.mlr.press/v162/zhmoginov22a.html>. 11

[74] Allan Zhou, Kaien Yang, Kaylee Burns, Adriano Cardace, Yiding Jiang, Samuel Sokota, J. Zico Kolter, and Chelsea Finn. Permutation equivariant neural functionals. In Alice Oh, Tristan Naumann, Amir Globerson, Kate Saenko, Moritz Hardt, and Sergey Levine, editors, *Advances in Neural Information Processing Systems 36: Annual Conference on Neural Information Processing Systems 2023, NeurIPS 2023, New Orleans, LA, USA, December 10 - 16, 2023*, 2023. URL [http://papers.nips.cc/paper\\_files/paper/2023/hash/4e9d8aeeab6120c3c83ccf95d4c211d3-Abstract-Conference.html](http://papers.nips.cc/paper_files/paper/2023/hash/4e9d8aeeab6120c3c83ccf95d4c211d3-Abstract-Conference.html). 12

[75] Allan Zhou, Kaien Yang, Yiding Jiang, Kaylee Burns, Winnie Xu, Samuel Sokota, J. Zico Kolter, and Chelsea Finn. Neural functional transformers. In Alice Oh, Tristan Naumann, Amir Globerson, Kate Saenko, Moritz Hardt, and Sergey Levine, editors, *Advances in Neural Information Processing Systems 36: Annual Conference on Neural Information Processing Systems 2023, NeurIPS 2023, New Orleans, LA, USA, December 10 - 16, 2023*, 2023. URL [http://papers.nips.cc/paper\\_files/paper/2023/hash/f4757db82a02eea015670eccaa605d5cc-Abstract-Conference.html](http://papers.nips.cc/paper_files/paper/2023/hash/f4757db82a02eea015670eccaa605d5cc-Abstract-Conference.html). 12

[76] Allan Zhou, Chelsea Finn, and James Harrison. Universal neural functionals. *CoRR*, abs/2402.05232, 2024. doi: 10.48550/ARXIV.2402.05232. URL <https://doi.org/10.48550/arXiv.2402.05232>. 12

## A Implementation Details and Hyperparameter Tuning

All our experiments are run on a single Nvidia A100 GPU, using a 10 GPU node.

### A.1 Instruction Tuning

Following [64], we tune the hyperparameters by fine-tuning the LLaMA-1 [55] model on the Alpaca52k dataset [] and use Alpaca-Eval v1.0 [31] with GPT-4 Turbo as the annotator for evaluation. Table 10 shows the hyperparameters used in our experiments. We base our training code on the implementation provided by [64] at <https://github.com/stanfordnlp/pyreft>. We report the final results by finetuning the Llama-2 model [56] using the Ultrafeedback dataset [9] and use and use Alpaca-Eval v1.0 [31] with GPT-4 as the annotator for evaluation. We report average results of 2 runs with seeds 42 and 43.

Hyperparameter	Value
Learning Rate	$5e^{-5}, 7.5e^{-5}, 1e^{-4}, 2.5e^{-4}, 5e^{-4}, 7.5e^{-4}, 1e^{-3}$
Rank	<b>16</b> , 32, 64, <u>128</u>
Optimizer	AdamW
Weight Decay	0.0
LR Scheduler	Linear
Warmup Ratio	0.0
Batch Size	4
Gradient Accumulation Steps	32
Epochs	12

Table 9: Hyperparameters used for the commonsense reasoning experiments. We only perform search over the learning rate and the rank, and choose the other hyperparameters from [64]. Bold faced and underlined pairs denote the final hyperparameters.

### A.2 Commonsense & Arithmetic Reasoning

Following [64], we tune the hyperparameters for commonsense and arithmetic reasoning by fine-tuning the LLaMA-1 model on the GSM8k dataset [8] using a separate validation set constructed from the training set. We fine-tune on the GSM8k for 12 epochs, but use 6 epochs for fine-tuning on the Commonsense170k as done in [64]. Table 10 shows the hyperparameters used in our experiments. We base our training code on the implementation provided by [64] at <https://github.com/stanfordnlp/pyreft>. We search for the hyperparameters using LLaMa-1 and use the same hyperparameters for Llama 2 and Llama 3 models. We perform hyperparameter search using the seed 42, and report the final results by averaging over three runs with seeds 42, 43, and 44.

Hyperparameter	Value
Learning Rate	$5e^{-5}, 7.5e^{-5}, 1e^{-4}, 2.5e^{-4}, 5e^{-4}, 7.5e^{-4}, 1e^{-3}$
Rank	16, 32, <u>64</u> , 128
Optimizer	AdamW
Weight Decay	0.0
LR Scheduler	Linear
Warmup Ratio	0.1
Batch Size	8
Gradient Accumulation Steps	4
Epochs	12 on GSM8k and Math10k, 6 on Commonsense170k

Table 10: Hyperparameters used for the commonsense reasoning experiments. We only perform search over the learning rate and the rank, and choose the other hyperparameters from [64]. The final hyperparameters are underlined.

### A.3 FGVC and VTAB Experiments

For all the experiments, we use ViT-B/16 model [12], which contains 12 transformer blocks, each with 12 heads in the Multi-Head Self-Attention (MHSA) blocks, and a dimension of 768. We use checkpoints from the model pretrained on the ImageNet21k [10] under the supervised training protocol provided by the `timm` package. For both VTAB and FGVC experiments, we use a hyperparameter search using the validation sets and use the training+validation data during the final run and report the results on the test sets. The hyperparameter search space used in our experiments is provided in Table 11. For the VTAB benchmark, we use the official splits provided by [68]. For the FGVC benchmark, we use the same train, validation and test splits as [53], *except for* Stanford Cars dataset [14]. Due to the unavailability of the dataset from the [original source](#), and the difference in the format of the data provided by the [updated source](#), we create our own training and validation split (with the same number of images as [53]) and use the official testing split.

Hyperparameter		Values
BitFit	Learning Rate	$1e^{-3}, 1.5e^{-3}, 2e^{-3}, 2.5e^{-3}, 5e^{-3}, 1e^{-2}$
	Weight Decay	0.0
VPT	Learning Rate	$1e^{-3}, 1.5e^{-3}, 2e^{-3}, 2.5e^{-3}, 5e^{-3}, 1e^{-2}$
	Weight Decay	0.0
	Num. Prompts	5
LoRA	Learning Rate	$1e^{-3}, 1.5e^{-3}, 2e^{-3}, 2.5e^{-3}, 5e^{-3}, 1e^{-2}$
	Weight Decay	0.01, 0.001, 0.0001, 0.0
	Rank $r$	8
GIFT	Learning Rate	$1e^{-4}, 2.5e^{-4}, 5e^{-4}, 1e^{-3}, 2.5e^{-3}, 5e^{-3}$
	Weight Decay	0.01, 0.001, 0.0001, 0.0
	Rank $r$	16
Optimizer	Optimizer	AdamW [38]
	LR Scheduler	Cosine
	Warmup Epochs	5
	Epochs	100
	Batch Size	32

Table 11: Hyperparameter search space used for GLUE experiments. During the search, we use 50 epoch for each experiment in the VTAB benchmark for 25 epochs for the FGVC benchmark due to computational constraints, and use 100 epochs in the final run with the selected hyperparameters

### A.4 GLUE Benchmark

For our experiments with the GLUE benchmarks, we use RoBERTa-Base and RoBERTa-Large models [37]. Table 12 shows the hyperparameters used in our experiments. We perform the hyperparameter search using a single seed, and use 5 seeds for the final run and report the median across them. We use the seed 42 for performing hyperparameter search and use 42, 43, 44, 45, 46 for the final runs. We observe that for RoBERTa-Large, the training is unstable for some seeds, and hence replace them. Following [19] and [26], we use the training split for training the models and report the results on the validation split.

Hyperparameters		SST-2	MRPC	CoLA	QNLI	RTE	STS-B
Optimizer		AdamW					
Warmup Ratio		0.06					
LR Scheduler		Linear					
Rank $r$		32					
Base	LR	$5e^{-4}$	$1e^{-3}$	$5e^{-4}$	$5e^{-4}$	$7.5e^{-4}$	$5e^{-4}$
	Weight Decay	0	0	$1e^{-4}$	$1e^{-2}$	$1e^{-3}$	$1e^{-3}$
	Epochs	60	30	80	25	160	80
	Batch Size	64					
Large	Max Seq. Len.	512					
	LR	$1e^{-3}$	$5e^{-4}$	$7.5e^{-4}$	$2.5e^{-4}$	$5e^{-4}$	$7.5e^{-4}$
	Weight Decay	$1e^{-2}$	$1e^{-4}$	$1e^{-2}$	0	$1e^{-2}$	0
	Epochs	10	40	40	20	40	20
Batch Size		128					
Max Seq. Len.		128					

Table 12: Hyperparameter search space used for GLUE experiments. Except for  $r$ , learning rate and weight decay, all the other hyperparameters have been taken from [26] due to computational constraints.

## B Generation Examples

### Commonsense Reasoning (WinoGrande)

Please choose the correct answer to fill in the blank to complete the given sentence: Sarah was a much better surgeon than Maria so \_ always got the easier cases.

Option1: Sarah Option2: Maria Answer format: option1/option2

Model	Response
LLaMA-1 7B (GIFT)	option1
Llama-2 7B (GIFT)	option2
Llama-3 7B (GIFT)	option2

### Commonsense Reasoning (OBQA)

Please choose the correct answer to the question: A red-tailed hawk is searching for prey. It is most likely to swoop down on

Answer1: an eagle Answer2: a cow Answer3: a gecko Answer4: a deer

Answer format: answer1/answer2/answer3/answer4

Model	Response
LLaMA-1 7B (GIFT)	answer4
Llama-2 7B (GIFT)	answer4
Llama-3 7B (GIFT)	answer3

### Arithmetic Reasoning (GSM8K)

A car in the fast lane is traveling at 60 miles/hour. A car in the slow lane is traveling at half that speed. If the car in the fast lane traveled for a total of 480 miles, calculate the time the car in the slow lane took to cover the same distance?

**Model****LLaMA-1 7B****Response**

Let's start by finding the speed of the car in the slow lane. We know that the car in the fast lane is traveling at 60 miles/hour, and the car in the slow lane is traveling at half that speed, which means:

$$\text{Speed of car in slow lane} = 0.5 \times 60 \text{ miles/hour} = 30 \text{ miles/hour}$$

Now we can use the formula:

$\text{Distance} = \text{Rate} \times \text{Time}$  We know that the car in the fast lane traveled for a total of 480 miles, so we can set up the equation:

$$480 \text{ miles} = \text{Rate} \times \text{Time}$$

We can substitute the speed of the car in the fast lane into the equation:  
 $480 \text{ miles} = 60 \text{ miles/hour} \times \text{Time}$

Now we can substitute the speed of the car in the slow lane into the equation:

$$480 \text{ miles} = 30 \text{ miles/hour} \times \text{Time}$$

We can solve for Time by dividing both sides by 30 miles/hour:

$$\text{Time} = 16 \text{ hours}$$

Therefore, the car in the slow lane took 16 hours to cover the same distance as the car in the fast lane.

List the layers of the TCP/IP model and for each layer identify one protocol.

**Model**  
**GIFT (r=128)**

**Response**

The TCP/IP (Transmission Control Protocol/Internet Protocol) model is a standard network architecture used to communicate between devices on the Internet. It consists of four main layers, which are as follows:

1. Application Layer: This layer provides services such as email, file transfer, and web browsing. The most common protocol at this layer is HTTP (Hypertext Transfer Protocol).
2. Transport Layer: This level handles data transmission between applications. The most common transport protocols include TCP (Transmission Control Protocol) and UDP (User Datagram Protocol).
3. Internet Layer: This is responsible for routing packets across the internet. The most common internet protocol at this layer is IP (Internet Protocol).
4. Network Interface Layer: This interface connects the computer to the physical network. The most common network interface protocol is Ethernet.

**GIFT (r=16)**

The TCP/IP (Transmission Control Protocol / Internet Protocol) model is a standard network architecture used to communicate between devices on the internet or any other computer network. It consists of four layers, each with its own set of protocols:

1. **Application Layer** - This layer provides services such as email, web browsing, file transfer, and remote login. The most common protocol at this layer is Hypertext Transfer Protocol (HTTP).
2. **Transport Layer** - It ensures reliable data delivery by segmenting messages into smaller units called segments and reassembling them at the receiving end. The main protocol here is Transmission Control Protocol (TCP).
3. **Internet Layer** - Also known as the Network Layer, it handles routing and forwarding of packets across multiple networks. The primary protocol in this layer is Internet Protocol (IP).
4. **Data Link Layer** - Responsible for establishing and maintaining connections between two hosts on a network. The most commonly used protocol at this level is Ethernet.

Here are some examples of protocols associated with each layer:

- Application Layer: HTTP, FTP, Telnet, SMTP, DNS, etc.
- Transport Layer: TCP, UDP
- Internet Layer: IPv4, IPv6
- Data Link Layer: Ethernet, Token Ring, FDDI, ATM, etc.

## Instruction Tuning (Alpaca-Eval) - Llama-2 7B

Write a pitch for a horror movie that plays on the island Sylt in northern Germany in the 19th century. Include fishermen and a sinister force that drives the inhabitants insane.

### Model GIFT (r=128)

#### Response

Title: "The Curse of Sylt"

Synopsis: A group of fishermen from the picturesque island of Sylt, located in Northern Germany, find themselves caught in a web of terror as they uncover a sinister force lurking beneath the surface of their tranquil community. As the men delve deeper into the mystery, they begin to experience strange visions and hear whispers in the night, leading them down a path of madness and despair. The island's inhabitants are driven to the brink of insanity by this malevolent force, which seems to have no end in sight. Can our heroes break free from its grasp before it's too late? Find out in "The Curse Of Sylt," a chilling tale of horror and suspense set against the backdrop of a beautiful but deadly island paradise.

### GIFT (r=16)

Title: "The Haunting of Sylt"

Synopsis: A group of fishermen from the small village of List on the remote island of Sylt, Germany, are plagued by a mysterious force that drives them to commit unspeakable acts of violence against their loved ones. As the villagers succumb to madness, they begin to suspect that something sinister lurks beneath the surface of the island's tranquil waters. Is it a curse? Or could there be a more sinister explanation for the chaos that has descended upon their once-peaceful community? Join us as we delve into the depths of this haunted island and discover the truth behind its dark secrets.

## C More Qualitative Results on the Interpretability of GIFT

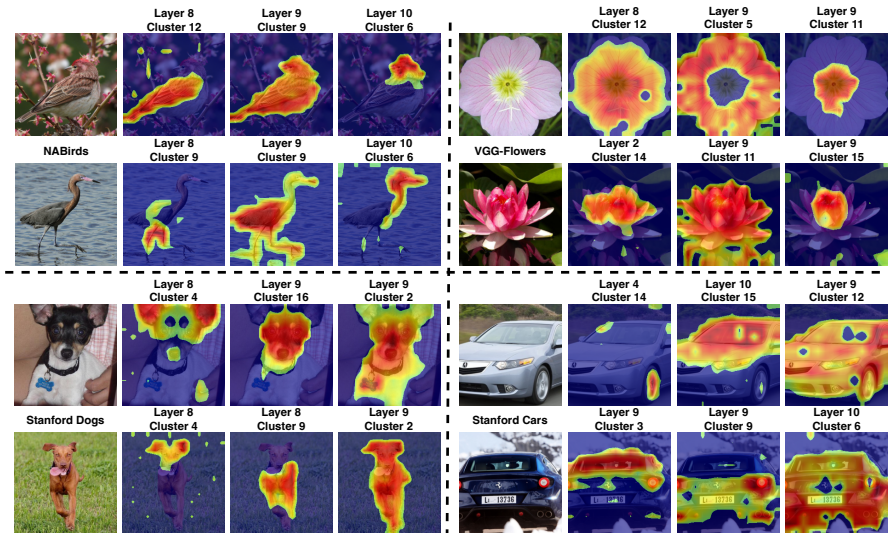


Figure 4: More examples of the visual interpretability of our two-linear-layer parameterized GIFT tested on the FGVC benchmark. We show examples of head, wings and legs of birds in the *top-left*, examples of flower petals in the *top-right*, examples of head, ears and legs of dogs in the *bottom-left*, and examples of tires, windshield and bumper of cars in the *bottom-right*.